AD_____

AWARD NUMBER: DAMD17-02-1-0438

TITLE: Breast Cancer in Context: New Tools and Paradigms for the Millennium

PRINCIPAL INVESTIGATOR: Mina J. Bissell, Ph.D.

CONTRACTING ORGANIZATION: Ernest O. Lawrence Berkeley National Laboratory
Berkeley, California 94720

REPORT DATE: July 2006

TYPE OF REPORT: Annual

PREPARED FOR: U.S. Army Medical Research and Materiel Command
Fort Detrick, Maryland 21702-5012

REPORT DOCUMENTATION PAGE

Form Approved
OMB No. 0704-0188

1. REPORT DATE *(DD-MM-YYYY)*	**2. REPORT TYPE**	**3. DATES COVERED** *(From - To)*
01-07-2006	Annual	1 Jul 2005 – 30 Jun 2006

4. TITLE AND SUBTITLE

Breast Cancer in Context: New Tools and Paradigms for the Millennium

5a. CONTRACT NUMBER

5b. GRANT NUMBER
DAMD17-02-1-0438

5c. PROGRAM ELEMENT NUMBER

6. AUTHOR(S)

Mina J. Bissell, Ph.D.

E-Mail: MJBissell@lbl.gov

5d. PROJECT NUMBER

5e. TASK NUMBER

5f. WORK UNIT NUMBER

7. PERFORMING ORGANIZATION NAME(S) AND ADDRESS(ES)

Ernest O. Lawrence Berkeley National Laboratory
Berkeley, California 94720

8. PERFORMING ORGANIZATION REPORT NUMBER

9. SPONSORING / MONITORING AGENCY NAME(S) AND ADDRESS(ES)
U.S. Army Medical Research and Materiel Command
Fort Detrick, Maryland 21702-5012

10. SPONSOR/MONITOR'S ACRONYM(S)

11. SPONSOR/MONITOR'S REPORT NUMBER(S)

12. DISTRIBUTION / AVAILABILITY STATEMENT
Approved for Public Release; Distribution Unlimited

13. SUPPLEMENTARY NOTES

14. ABSTRACT

We hypothesize that breast tumors are capable of multiple differentiation pathways. A finite number of interconnected pathways establish homeostasis in normal tissues which, if still functional in tumors, may be manipulated. Our goal is to characterize -51 breast cancer cell lines with known genomic profiles utilizing a robust 3-dimensional assay with laminin-rich extracellular matrix (3D IrECM). In this assay non-malignant mammary epithelial cells form acinar structures whereby cells growth arrest, polarize and form a central lumen while tumorigenic cells continue to proliferate and form a disorganized mass. In this assay, treatment of tumorigenic cells with various signaling inhibitors alone or in combination phenotypically "reverts" or kills cancer cells. To date, the majority of the tumor lines have been obtained and grouped according to their morphology in 3D IrECM. Refined analysis identified six distinct morphologies termed round, round mass, irregular mass, grape-like, grape-like stellate and invasive stellate. Twenty-six cell lines have been characterized by gene expression and proteomic profiles of selected signaling pathways. We are analyzing these expression profiles to identify common signaling themes and/or morphological regulators as well as performing studies correlating morphology and expression profiles with response to Herceptin and other therapeutic agents.

15. SUBJECT TERMS
Breast Cancer

16. SECURITY CLASSIFICATION OF:			**17. LIMITATION OF ABSTRACT**	**18. NUMBER OF PAGES**	**19a. NAME OF RESPONSIBLE PERSON**
a. REPORT	**b. ABSTRACT**	**c. THIS PAGE**			USAMRMC
U	U	U	UU	31	**19b. TELEPHONE NUMBER** *(include area code)*

Table of Contents

Innovator Award 2006 Annual Report
Breast Cancer in Context: New Tools and Paradigms for the Millennium

Introduction

Hypothesis

Breast tumors are capable of multiple differentiation pathways. As a finite number of interconnected pathways establish homeostasis in normal tissues, these pathways, if still functional, could be manipulated in tumors.

Background

This project was designed to gain a broad picture of how the microenvironment influences the development of cancer and how manipulation of microenvironment-cell interactions could be used to identify the interconnected pathways that may be potential therapeutic targets. Finally, we hypothesize that the 3D assay which was developed in this laboratory lends itself to a better assay for testing single or multiple drugs.

Microenvironmental regulators, including the extracellular matrix (ECM), its receptors, most notably integrins, cell-cell, and stromal-epithelial interactions, are critical determinants of both homeostasis and malignancy. How abnormal environments can contribute to genomic instability, and conversely, how an overt malignant genome could be controlled by seemingly simple manipulations of the extracellular milieu or surface receptors, have only begun to be explored; our challenge is to reconcile the mutation paradigm with the role of the microenvironment ("context") to create a unified theory of cancer.

To this end we will characterize ~60 breast cancer cell lines with known genomic profiles (CGH analysis), utilizing a robust three dimensional laminin-rich extracellular matrix assay (3D lrECM). In this assay non-malignant mammary epithelial cells form acinar, *in vivo*-like structures in which the cells withdraw from the cell cycle, polarize, and form a central lumen whereas tumorigenic cells continue to proliferate and form a disorganized mass. Treatment of the tumorigenic cells with a variety of signaling inhibitors, either single or in combination, are capable of either phenotypically reverting "normal" structures or killing a variety of breast cancer cell lines in the 3D lrECM assay.

Body

Our collaborator, Joe Gray, and his laboratory in conjunction with the UCSF Breast Cancer SPORE have collected over 64 breast cancer cell lines. His group has characterized the genomic profile for each of the cell lines by comparative genomic hybridization (CGH) as well as by the RNA expression profile of these cells cultured on tissue culture plastic in two dimensions (2D), utilizing Affymetrix technology. We have proposed to look at the entire panel of cell lines in our 3D lrECM assay. In the past year they have reduced the number of breast cancer cell lines they

propose to work with to approximately 51, primarily due to unfavorable growth properties of some cell lines. Our group is now also focusing on these 51 cell lines in particular.

In the previous review period, we added the immunolocalization of actin structure to our morphological analysis. This allowed us to refine our definitions to six distinct morphologies: round, round mass, irregular mass, grape-like, grape-like stellate and invasive stellate (Table 1; Figure 1). As we have increased the number of cell lines categorized in this manner, we have found fair variety in the morphologies presented by breast cancer cell lines grown in 3D lrECM and, depending on the cell line, a certain degree of heterogeneity within the lines themselves. Our current rules delineating the morphological categories are described in Table 2; however we consider these categories flexible as we continue to learn about the behavior of this panel of cell lines in 3D lrECM.

We are also continuing to collect proteomic and proliferation data on these cell lines. As of yet, there is no obvious correlation either between proliferation and morphology or protein expression of the set of molecules investigated with morphology, with the exception of the lack of E-cadherin in the invasive stellate cell lines, which we reported in 2004 and continues to describe our data to this date.

Towards the aim of automating and standardizing our morphological categorization rules, we have begun collaborating with Bahram Parvin, a bioinformatician at LBNL with extensive experience in quantitative image analysis. We have provided him phase images and confocal sections of F-actin and nuclear staining of various cancer cell lines in 3D lrECM with the goal of being able to feed images into a computational system that would objectively designate a morphological grouping based on predetermined rules.

Expression profiling

As described previously, LBNL has been in the process of establishing an expression core utilizing a high throughput 96 well Affymetrix format (HTA) which resulted in our having to generate a new set of data on the HTA format. In last year's report we described expression data from the 16 cell lines, containing representatives from each of the 6 morphological groups, of which we had the opportunity to re-run on the HTA system. Although we did not anticipate any further delays in acquiring expression data, there were in fact two major stoppage points in throughput due to system validations. However, to this date we have baseline expression data on 26 cell lines and have four more cell lines in the pipeline.

GeneSpring analysis software was used to perform hierarchical cluster analysis of the baseline expression profiles of the 26 cell lines and identified that the cell lines examined thus far fall into three major clusters, similarly as to when only 16 cell lines were analyzed (Figure 2).

To determine whether the groups defined by the 3D clustering analysis were similar to the 2D classifications (Luminal, Basal10 and Basal231) identified by the Gray laboratory, we overlaid the respective cell line's 2D classification onto our 3D groups and found that two of the three classes (Luminal and Basal 231) still correlated with two of our three clusters as when we had data on ten fewer cell lines (Figure 3). Additionally when the same clusters are colored by their

distinct 3D morphology we find that the distinct cell morphologies are mostly clustered together within the groups (Figure 4, top panel). If the six 3D morphological categories are collapsed into three general groupings, the clustering becomes somewhat cleaner (Figure 4, bottom panel). As reported previously with fewer cell lines, the three large clusters appear to group the cell lines by their perceived aggressiveness i.e. round, grape and mass are in one cluster and would be expected to be less aggressive than the stellate cell lines found in the second cluster. The third cluster contains the in vitro derived HMT-3522 progression series (non-malignant S1 and malignant T4), the normal cell line MCF12A, and the tumor cell lines BT549, MCF-7 and HCC-1500. As the malignant HMT-3522 T4 cell line was derived directly from the non-malignant S1 cell line by selection for EGF independent growth and ability to form tumors in nude mice, they may reflect an earlier stage of tumorigenesis than those derived from actual human tumors. The HCC-1500 cell line is near diploid, her2/neu- and p53 positive which are thought to be hallmarks of a less aggressive breast cancer. The ER-positive MCF-7 cell line is also known to be a less aggressive tumor cell line and in xenograft models, often requires estradiol supplementation for tumor growth. Therefore this cluster may contain cell lines in an earlier stage of tumorigenesis. The one outlier is BT549, a highly aneuploid and metastatic cell line. However, when clustering is performed with tumor cell lines only (S1 and MCF12A removed), BT549 moves away from this cluster and into the stellate cluster. Further analysis is needed to determine whether this is a meaningful result or a quirk of the clustering algorithm.

These data indicate that the 3D analysis appears to provide a finer delineation or sub-categorization of the cell lines than can be obtained from the 2D expression profiles. We are also heartened that as our sample size has increased from 16 to 26 cell lines that the same major clusters have been maintained. However, as Figure 4 shows, we may have to maintain flexibility in our 3D morphological categorizations as we do not currently know whether it is meaningful in this context to differentiate between round and round mass as we now define these categories or whether as we accumulate data on additional cell lines, we will learn which lines have physiological significance.

We have also begun to interrogate the differences in the gene expression profiles between matched cell lines in 2D and 3D (Figure 5). This cluster also includes 3 sets of xenograft data, provided to us by Byron Hann, UCSF. In this analysis there is a cluster of genes which is strikingly downregulated in 2D in comparison to 3D and xenograft samples. We performed gene ontology analyses on this gene list using GOstat and found that in this group of genes, membrane proteins were significantly overrepresented while the RNA binding, biopolymer metabolism and ubiquitin cycle classes were underrepresented (Table 3). We will continue performing these analyses as we build our expression data set and also acquire more matched xenograft expression data (either from collaborators or self-generated, as described in Task 5) and will validate molecules and pathways of interest.

Therapeutic Response

In previous years we had focused on the response of cell lines of differing morphologies to signaling inhibitors targeting pathways including EGFR-MAPK and Akt. However, we found that treatment of the cell lines with these inhibitors at most resulted in a modest decrease in proliferation. Some more recent data testing EGFR inhibition in a subset of these cell lines gave

similar results (Paraic Kenny, personal communication). In contrast, in data presented in last year's report, we found that AIIB2, a beta1 integrin function blocking antibody, dramatically inhibited proliferation in 4 cell lines tested (Figure 6b). In this past year, our lab has published data, supported by this award, showing that blocking beta1 integrin in vitro and in xenograft animal models can induce apoptosis and decreased proliferation in a tumor depending on which breast cancer cell line was tested and therefore that AIIB2 has promise as a potential therapeutic (Appendix A, Park et al, 2006). We also treated cell lines with Herceptin, the clinical therapeutic which blocks ErbB2, and found that it had little effect by morphology or cell proliferation on cell lines tested with the exception of BT474 (Figure 6c; Figure 7, bottom panel).

We have now analyzed the expression data from this experiment (Figure 7, top panel). As predicted by the morphological and cell proliferation response data, we find that in all cell lines tested, the expression profiles of the AIIB2 treated cells are the most unlike the controls (BT474 AIIB2 data is not available because the growth inhibition was so significant that not enough RNA could be collected for analysis). By expression profile, Herceptin had an effect on both BT474 and AU565. Although both cell lines are ErbB2 overexpressers, we noted before that only BT474 showed a response in terms of cell proliferation or colony size (Figure 7, bottom panel). However this data shows that, although modest, Herceptin may have had an effect on AU565 as we would expect from the protein data. The other ErbB2 overexpressing cell line tested, SKBR3, interestingly shows little to no effect by expression profile as a result of Herceptin treatment. However, there was a significant decrease in cell proliferation. This suggests either that ErbB2 blocking affects ErbB2 overexpressers in different manners, for example, there is an enhanced feedback loop to transcription in BT474 as compared to SKBR3, or simply that the majority of response to Herceptin is post-transcriptional. The case of AU565 also suggests that simple overexpression of ErbB2 may not necessarily be predictive of response to Herceptin. We also note that in the cell lines that do not respond at all to Herceptin (T47D, MDA-MB-231, T4), the IgG and Herceptin treated samples cluster together, perhaps indicating some nonspecific IgG effect of Herceptin.

Another result of interest in this experiment was the robust inhibition of the stellate phenotype of MDA-MB-231 by AIIB2. We then investigated whether other stellate cell lines responded to AIIB2 in this manner. Of four additional cell lines tested, two of which are categorized as grape-like stellate (MDA-MB-436; BT549) and two of which are invasive stellate (BT20; HS578T), three cell lines responded in a similar manner to AIIB2 as MDA-MB-231 (Figure 8). Interestingly, although morphological invasiveness of HS578T was decreased upon AIIB2 treatment, it was not almost completely inhibited as it was in the other cell lines. We wish to repeat this experiment with two additional stellate cell lines now characterized and to perform expression profiling in order to parse the differential response of HS578T and any additional cell lines to AIIB2.

We will also examine the expression profiles of all AIIB2 treated cells to determine if there are complements of genes which have similar expression profiles in cells which do respond and do not respond to blocking beta1 integrin but will await the larger sample numbers before performing analyses. We will characterize these genes using GO ontological characteristics and pathway analysis.

Although in our original statement of work we proposed to first identify reversion requirements of as many of the panel of cancer cell lines as possible (Task 2) and then to characterize the functional consequences of reversion (Task 4), our data has shown that the vast majority of these cell lines do not respond to signaling inhibition in the manner in which we have described reversion in the T4 cell line (Weaver et al, 1997; Wang et al, 2002). In other words, Tasks 2 and 4 were proposed based on our work with the HMT-3522 series and our findings that targeting individual signaling pathways in the T4 cells caused a phenotypic reversion with the reintroduction of nuclear organization and polarity. However, we are finding that T4 cells may represent an earlier stage in transformation as compared to many of the other cancer cell lines in our panel. Therefore, in order to redirect our focus on the identification of predictors of therapeutic response, we will continue to pursue the effects of blocking the beta1 integrin signaling pathways. We will also continue to investigate the effects of blocking the ErbB2 pathway, although we have not found very much effect in the 3D lrECM environment. If time permits we would also like to pursue combinatorial treatments of inhibitors of the EGFR-MAPK and Akt pathways as it is likely that tumor cell lines require perturbation at multiple signaling levels to achieve a reverted-like phenotype. We have found that each individual cell line is quite particular unto itself, and that identifying reversion requirements across the panel is non-trivial. Therefore it is more productive long-term to perform several small scale screens against inhibitors shown to have some morphological effect and then performing larger scale experiments to fulfill the goals of Task 4. We will focus on completing Tasks 4b and 4c, and Task 4d if we feel the time-lapse microscopy information would be informative to the end goal. We will address Task 4a if time and funds permit.

Key Research Accomplishments

3D morphologies may correlate with stage of tumor progression.
3D expression profiles may allow for identification of subtle differences between cell lines which are not obvious from 2D expression analysis.
Preliminary data suggest the differing morphologies may have different responses to therapeutic agents.
Beta1 integrin inhibition inhibits the invasive phenotype of the majority of stellate cell lines.

Reportable Outcomes

This award supported the publication of the following manuscript: Park CC, Zhang H, Pallavicini M, Gray JW, Baehner F, Park CJ, Bissell MJ (2006). β1 Integrin Inhibitory Antibody Induces Apoptosis of Breast Cancer Cells, Inhibits Growth, and Distinguishes Malignant from Normal Phenotype in Three Dimensional Cultures and In vivo. Cancer Research Feb 1;66(3):1526-35
Data from this project was presented in a poster at the annual American Society for Cell Biology meeting in December 2005.
Data from this project was used in a funding application to the National Institutes of Health Tumor Microenvironment Network U54 in May 2006.

Conclusions

We are continuing to build an extensive collection of morphological, proliferation, mRNA and protein expression data on a panel of breast cell lines in 3D lrECM and have full datasets on 26 cell lines to date. Bioinformatic analysis of genes which were identified as statically different based on morphology identified cell line clusters which appear to correlate with the stage of tumorigenesis. We have shown differences in therapeutic response amongst individual cell lines with differing morphologies and expression profile analysis suggests there are sets of genes which may correlate with response. In the coming year we will continue to accrue data and perform multivariant PCA analyses to build a predictive model of the key differences between behavior and therapeutic response of cell lines in 2D and 3D lrECM environments.

References

Park CC, Zhang H, Pallavicini M, Gray JW, Baehner F, Park CJ, Bissell MJ (2006). β1 Integrin Inhibitory Antibody Induces Apoptosis of Breast Cancer Cells, Inhibits Growth, and Distinguishes Malignant from Normal Phenotype in Three Dimensional Cultures and In vivo. Cancer Res. 66(3):1526-35.

Wang F, Hansen RK, Radisky D, Yoneda T, Barcellos-Hoff MH, Petersen OW, Turley EA and Bissell MJ (2002). Phenotypic Reversion or Death of Cancer Cells by Altering Signaling Pathways in Three-Dimensional Contexts. J. Nat'l Cancer Inst. 94(19):1494-1503.

Weaver VM, Petersen OW, Wang F, Larabell CA, Briand P, Damsky C, Bissell MJ (1997). Reversion of the malignant phenotype of human breast cells in three-dimensional culture and in vivo by integrin blocking antibodies. J. Cell Biol. 137(1):231-45.

Supporting Data

Morphology	Cell Lines	
Round	600 MPE	MDA-MB-415
	S1	MCF12A
	SUM 225CWN	
Round Mass	BT474	MCF7
	HCC-1569	HCC-1500
	HCC-202	SUM 52PE
	HCC-70	T4
	BT 483	AU-565
Irregular Mass	T47D	ZR-75-30
Grape-like	CAMA-1	SUM 149PT
	MDA-MB-468	ZR-75-1
	SKBR3	UACC-812
	MDA-MB-361	MDA-MB-453
	ZR-75-B	SUM 185PE
Grape-like Stellate	BT549	MDA-MB-436
Invasive Stellate	BT20	MDA-MB-157
	HS 578 T	MDA-MB-231
	HBL100	

Table 1. Morphological categorizations of breast cell lines cultured for 4 days in the 3D lrECM assay. Although there is some variance within categories, all cell lines can be grossly classified into six distinct morphological classes.

	Colony Morphology by Phase Contrast	Actin/Nuclei Organization
Round	Smooth, round outline	Nuclei organized with robust cell-cell contacts and cortical actin
Round Mass	Round outline	Nuclei disorganized with robust cell-cell contacts and cortical actin
Irregular Mass	Irregular outline	Nuclei disorganized with robust cell-cell contacts and cortical actin
Grape-like	Grape-like structure*	Nuclei disorganized with poor cell-cell contacts (grape-like in appearance) and cortical actin
Grape-like Stellate	Grape-like structure with some stellate projections	Nuclei disorganized with varying degrees of cell-cell contacts and some cortical actin; stellate projections do not contain nuclei
Invasive Stellate	Invasive branch-like structure	Nuclei disorganized with varying degrees of cell-cell contacts (grape-like in appearance) and some cortical actin; stellate projections often contain nuclei

Table 2. Rules governing morphological characterization. Although we currently make these distinctions between groups, they may also be collapsed into more general categories.

Best GOs	GO term	Genes	Count	Total	P-Value
			162	10884	
GO:0031224	intrinsic to membrane	ITM2B GP5 INSIG1 MTDH SERINC1 TNFRSF7 APP BCAP29 NCKAP1 SLCO5A1 CD52 SSR1 HIATL1 IPO7 SPPL2B	15	2651	0.00499
GO:0016021	integral to membrane	ITM2B GP5 INSIG1 MTDH SERINC1 TNFRSF7 APP BCAP29 NCKAP1 SLCO5A1 CD52 SSR1 HIATL1 IPO7 SPPL2B	15	2644	0.00499
GO:0003723	RNA binding	EIF1AX SFRS3 HNRPD RPS4Y1 FUSIP1 EIF4E RPL18 RBM25 SNRPA1 SON RPL27A SSB DGCR8 HRB2 HNRPA1 DDX3X STAU1	17	441	0.0207
GO:0016020	membrane	PGF GP5 BCAN MTDH C14ORF108 TNFRSF7 NDUFA5 APP BCAP29 SLCO5A1 CD52 HIATL1 ITM2B SEC24A INSIG1 MRPL19 ZFYVE16 SERINC1 GORASP2 OLFM1 PTP4A1 APC2 NCKAP1 LGALS4 YME1L1 SSR1 IPO7 SPPL2B MTFR1	29	3486	0.0341
GO:0043283	biopolymer metabolism	SET SFRS3 PRKAR1A HUS1 RAD21 ARIH1 KIAA0368 MAP4K3 CSPG6 RBM25 UBE1DC1 FBXO5 TTLL3 CDK10 STK3 ATRX DGCR8 HNRPA1 STK16 PTP4A1 SKP1A RNF11 PRPF4B YME1L1 SENP6 UBE2D1 HNRPD H2AFZ FUSIP1 PIAS1 UFM1 QTRTD1 SNRPA1 WWP1 PPP2R3A PPIG SSB ADAMTS2 HRB2 TSN MORF4L1 CLK1 RBBP6 PCYOX1 UBE3A DBR1 XRCC6	47	1972	0.0683
GO:0006512	ubiquitin cycle	FBXO5 SENP6 UBE2D1 ARIH1 SKP1A RNF11 RBBP6 PIAS1 UFM1 UBE3A WWP1 UBE1DC1	12	256	0.0683

Table 3. Gene ontology analysis of genes downregulated in 2D vs. 3D and xenograft. The gene cluster highlighted in Figure 5 was analyzed by GOstat (http://gostat.wehi.edu.au/) with p-value <0.01 and Benjamini multiple testing correction. All overrepresented (red p-values) and underrepresented (green p-values) gene ontologies are shown.

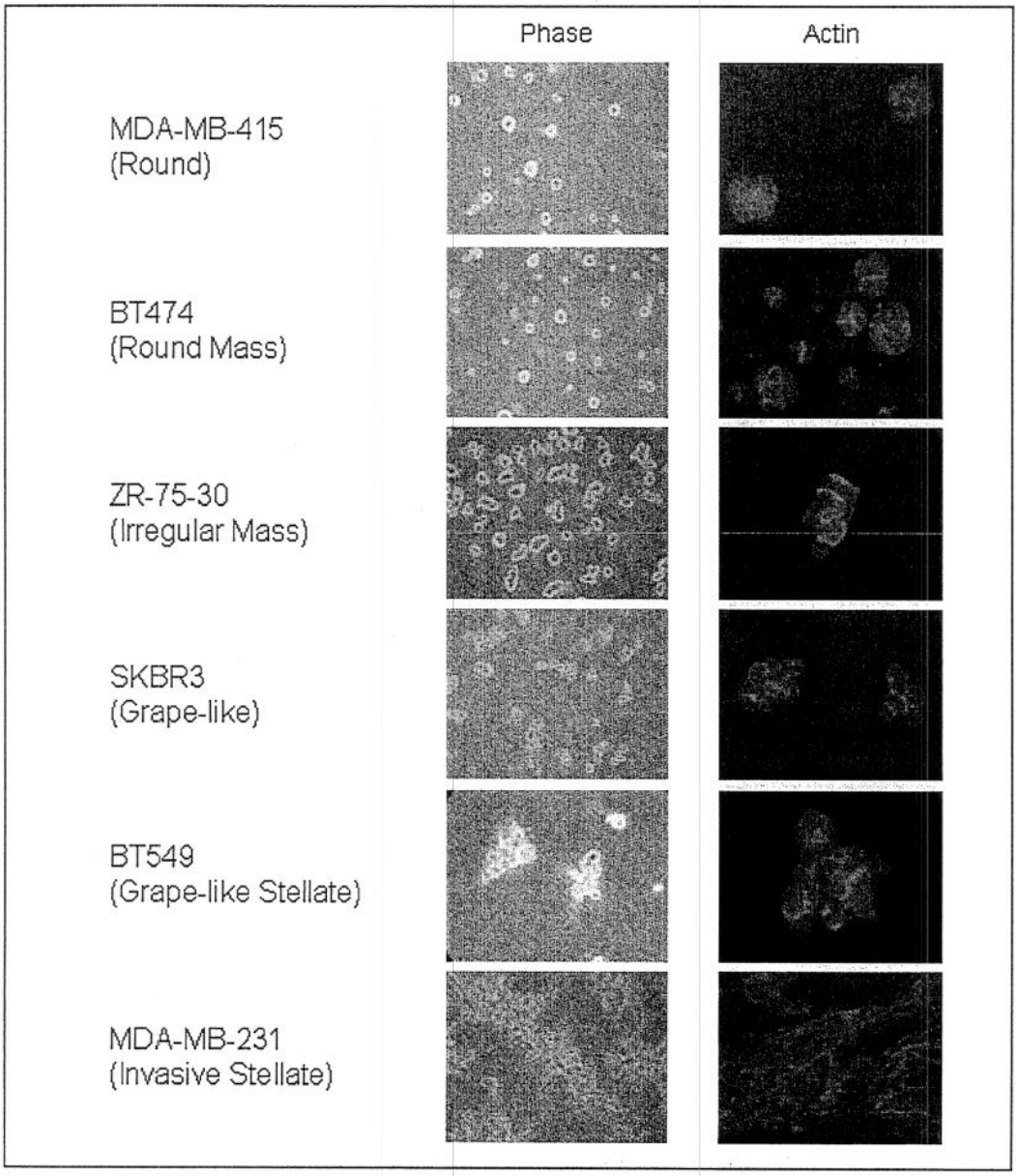

Figure 1. Morphological characterization of breast cell lines. When cultured on top of 3D lrECM with 5% lrECM drip for 4 days, breast cancer cell lines have differing morphologies which may be broken into 6 categories. Representative morphologies are shown by phase contrast (left column) and confocal sections of F-actin staining (right column, not to scale).

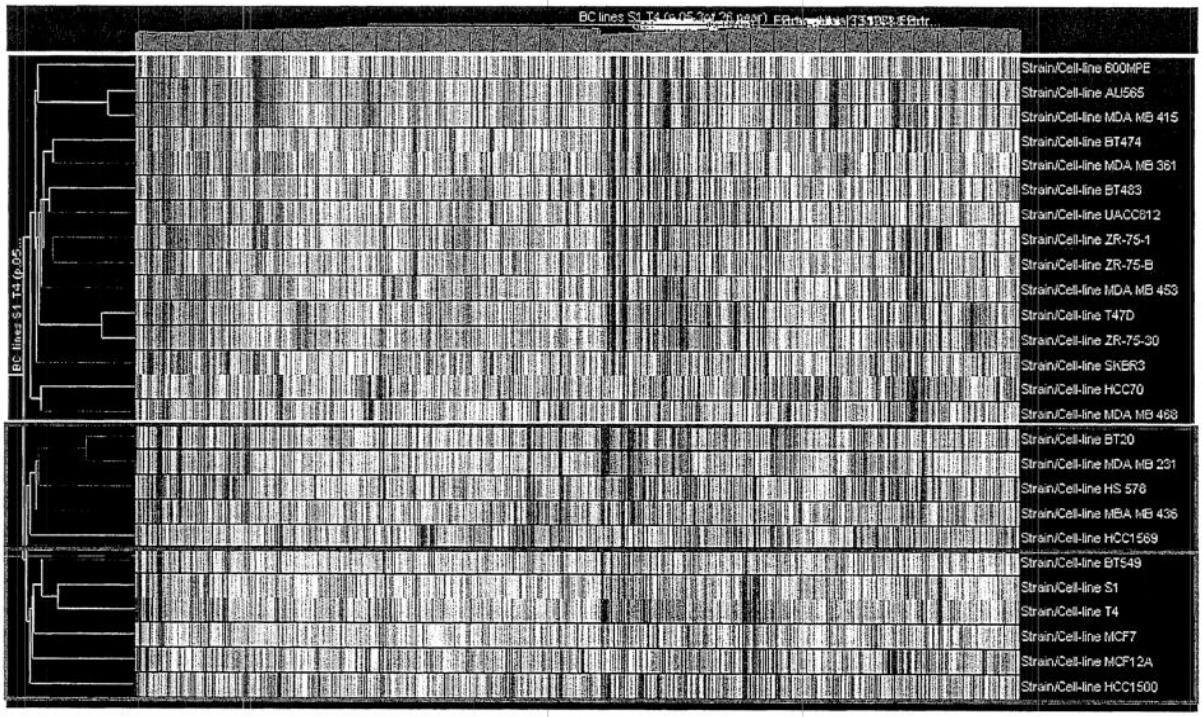

Figure 2. RNA isolated from 26 different cell lines cultured for four days on 3D lrECM was hybridized to the HTA U133A Affymetrix chip. Hierarchical clustering was performed using Genespring software using genes based on ANOVA with p-value <0.05 correlated with experimental parameter "Morphology." Clusters are condition trees with cell lines "colored" by morphology. All cell lines fall into three main clusters.

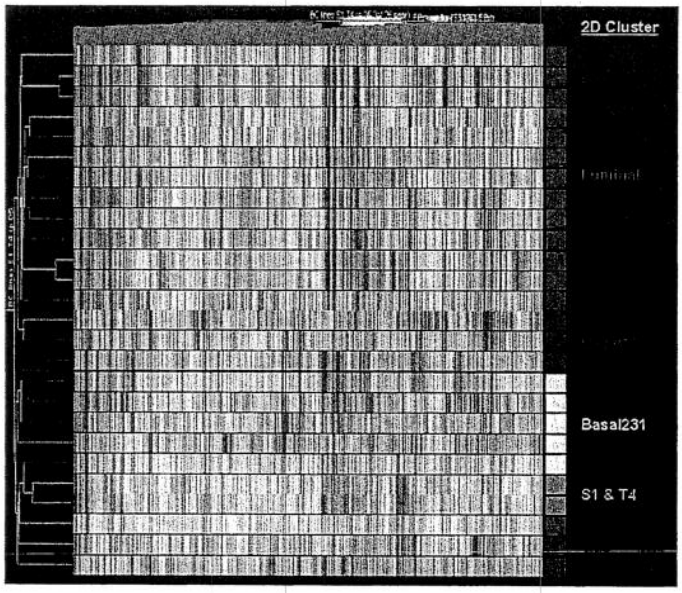

Figure 3. Hierarchical clusters of 3D profiles shown in Figure 2 are colored by their 2D expression profile classification.

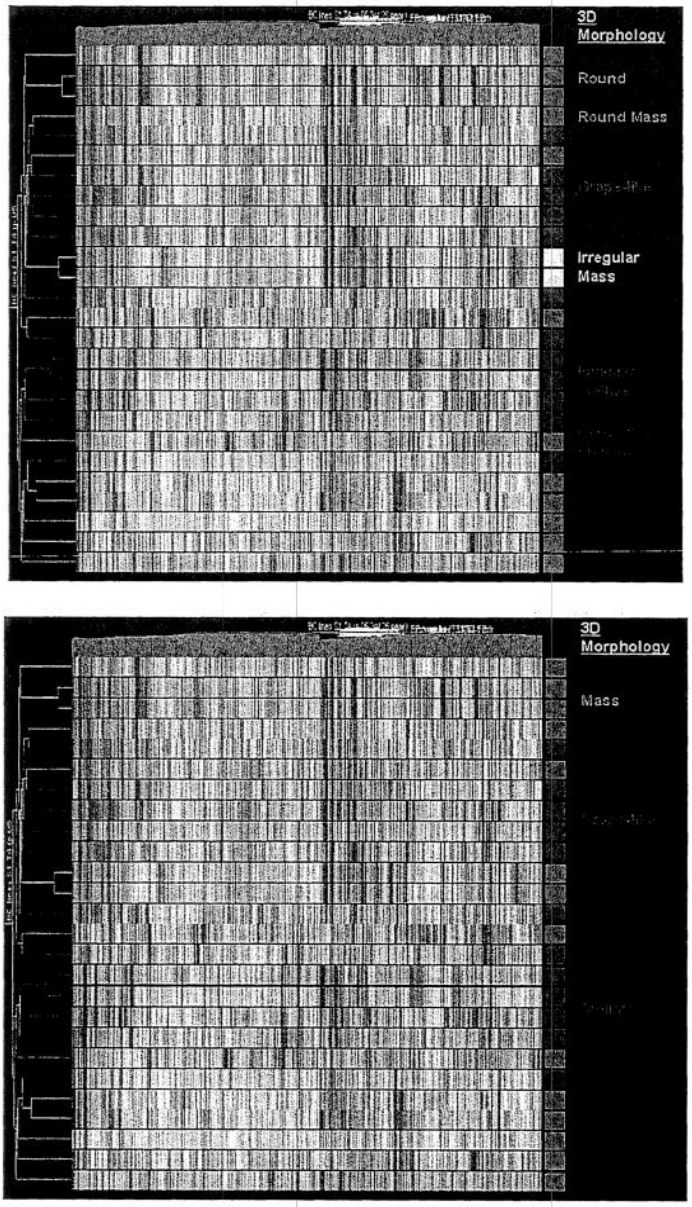

Figure 4. (Top) Hierarchical clusters of 3D profiles shown in Figure 2 are colored by their 3D morphology. (Bottom) The same clusters are shown with the six 3D morphologies collapsed into three generalized categories.

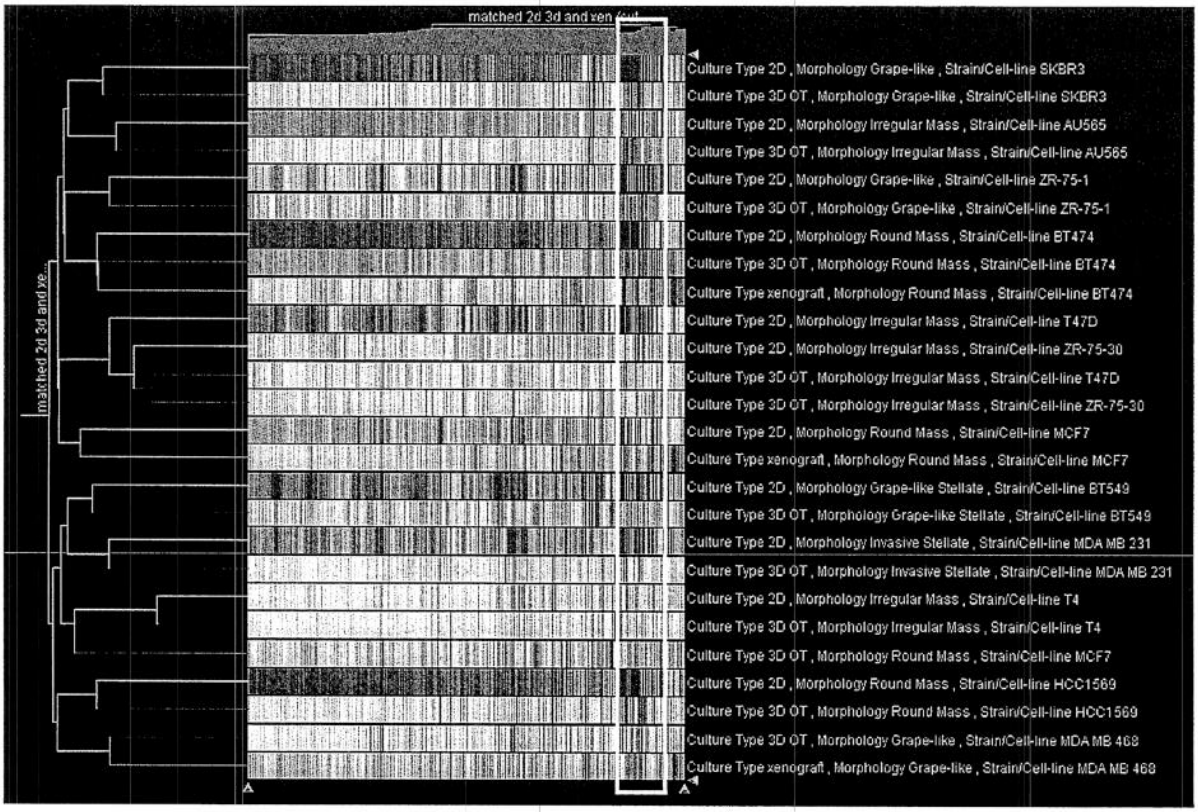

Figure 5. Hierarchical clustering was performed using Genespring software using genes based on ANOVA with p-value <0.05 correlated with experimental parameter "Culture Type" and not with "Strain/Cell-line" or "Morphology." Clusters are condition trees with cell lines "colored" by culture type. The gene cluster outlined was analyzed due to its significant degree of downregulation in the 2D samples as compared to matched 3D and xenograft samples.

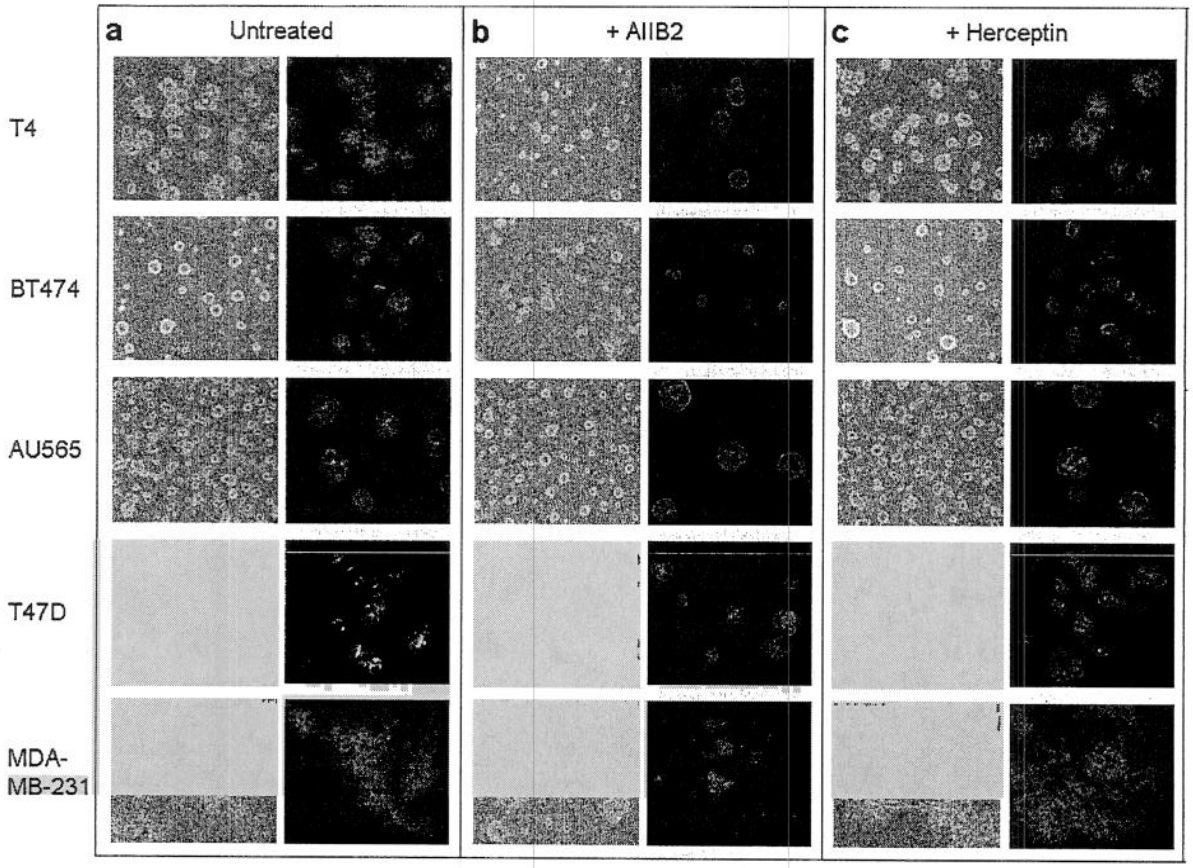

Figure 6. Perturbation of signalling pathways in breast cancer cell lines. a-c, Phase contrast (left column) and confocal sections of F-actin staining (right column) of 3D structures of cell lines (T4, BT474, AU565, T47D, MDA-MB-231) cultured on top of lrECM with 5% lrECM drip for 4 days, untreated (a), treated with AIIB2, a b1 integrin blocking antibody (b), or treated with Herceptin, an ErbB2 blocking antibody (c).

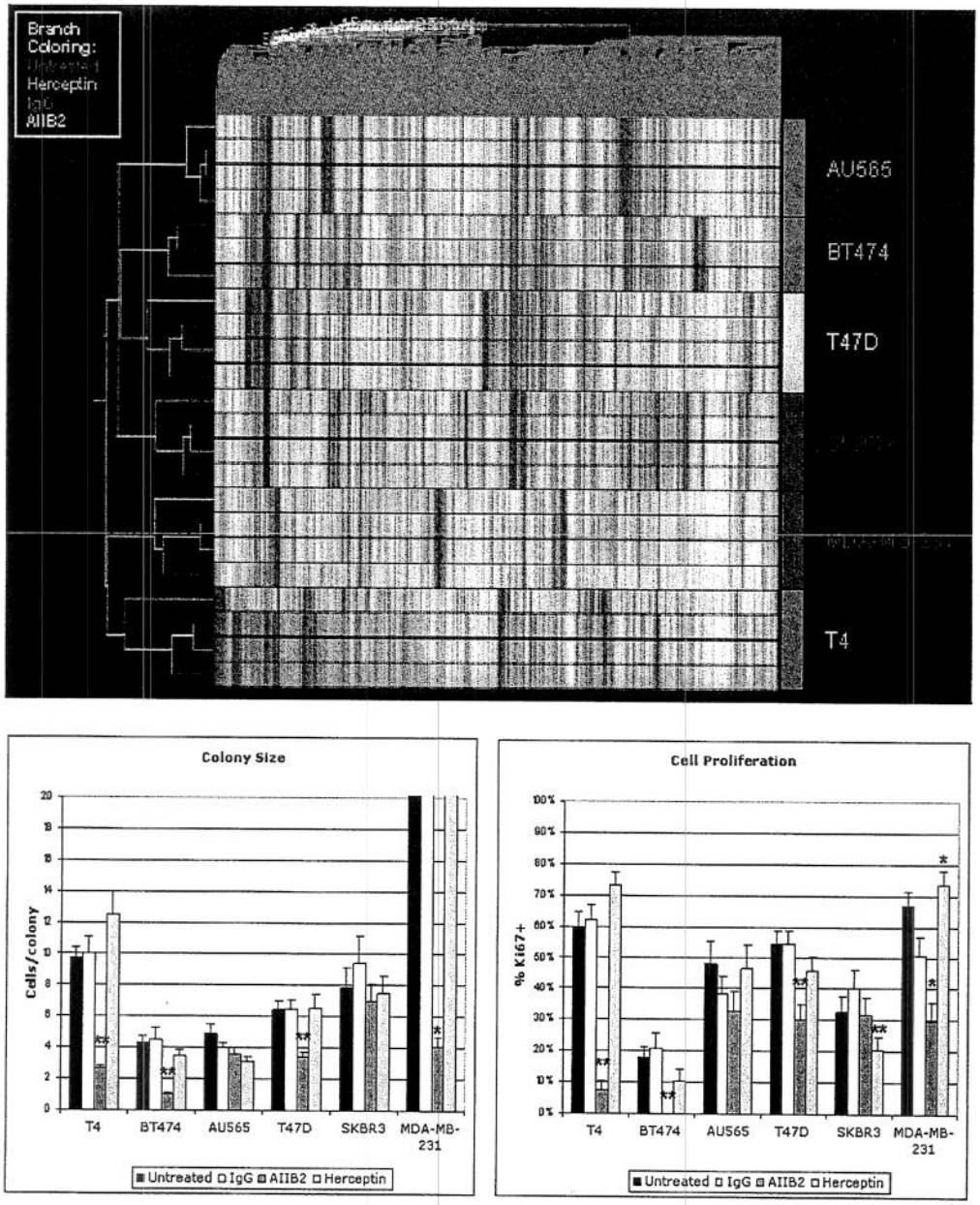

Figure 7. (Top) Hierarchical clustering of expression data from experiment depicted in Figure 6 using genes with p-value <0.05 in at least one condition. Branches are colored by inhibitor treatment and cell lines are indicated and colored by morphology to the right of the tree. (Bottom) Colony sizes and proliferation rates of cell lines subject to treatments in Figure 6. Colony size is measured as average number of cells per colony. Proliferation rate is measured as average number of Ki67-positive cells per colony. One asterisk indicates $p < 0.05$; two asterisks reflect $p < 0.01$, both in comparison to respective IgG controls. Error bars reflect standard error.

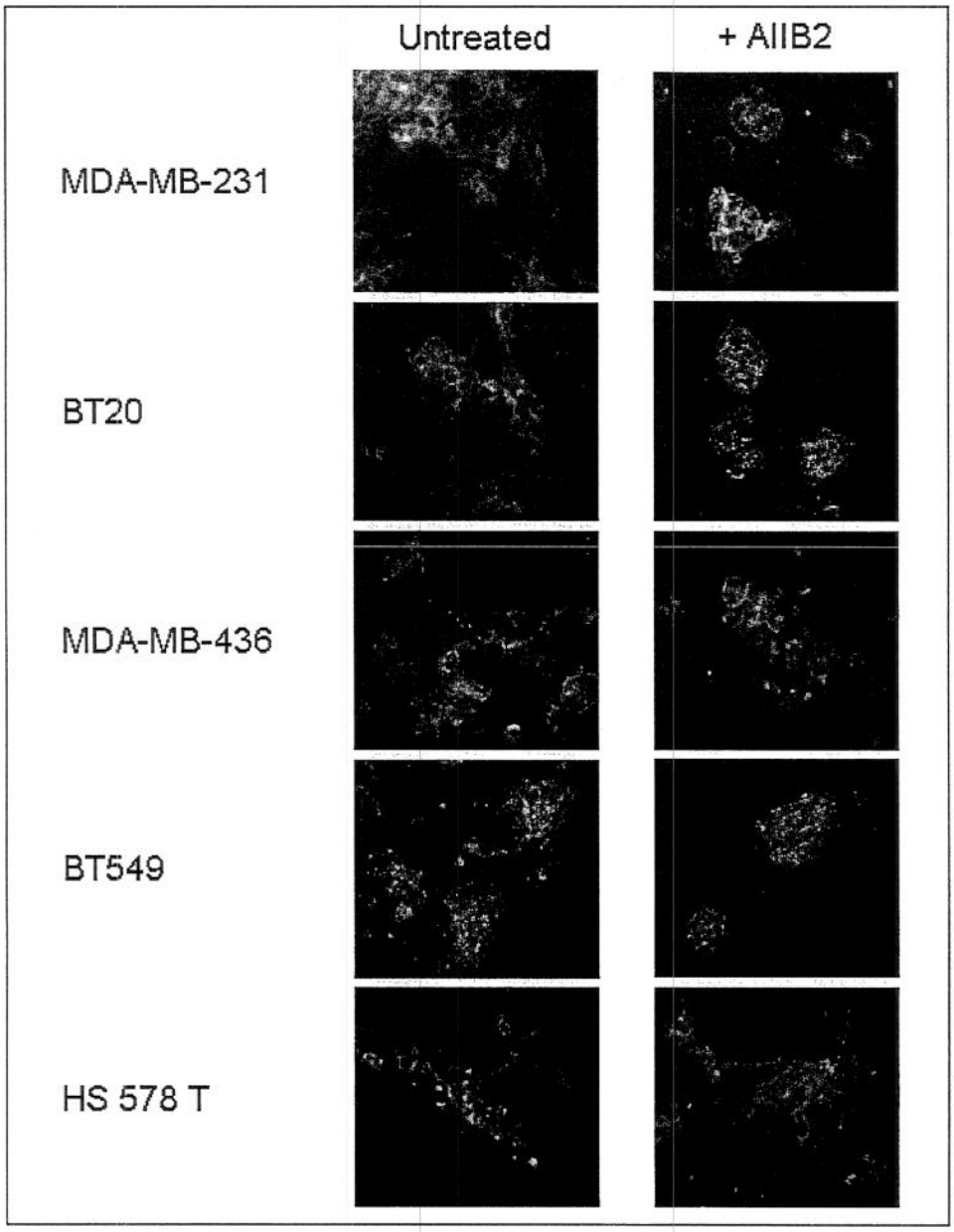

Figure 8. Three invasive stellate (MDA-MB-231, BT20, HS 578 T) and two grape-like stellate (MDA-MB-436, BT459) cell lines were treated with AIIB2. Z-projections of confocal stacks of F-actin staining are shown. The morphological invasiveness of all cell lines is almost completely inhibited by AIIB2, with the exception of HS 578 T.

Appendices

Appendix A

Park CC, Zhang H, Pallavicini M, Gray JW, Baehner F, Park CJ, Bissell MJ (2006). β1 Integrin Inhibitory Antibody Induces Apoptosis of Breast Cancer Cells, Inhibits Growth, and Distinguishes Malignant from Normal Phenotype in Three Dimensional Cultures and In vivo. Cancer Research Feb 1;66(3):1526-35

β_1 Integrin Inhibitory Antibody Induces Apoptosis of Breast Cancer Cells, Inhibits Growth, and Distinguishes Malignant from Normal Phenotype in Three Dimensional Cultures and *In vivo*

Catherine C. Park,[1] Hui Zhang,[3] Maria Pallavicini,[4] Joe W. Gray,[3] Frederick Baehner,[2] Chong J. Park,[5] and Mina J. Bissell[3]

Departments of [1]Radiation Oncology and [2]Pathology, University of California, San Francisco, California; [3]Life Sciences Division, Ernest Orlando Lawrence Berkeley National Laboratory, Berkeley, California; [4]School of Natural Sciences, University of California, Merced, California; and [5]Department of Mathematics and Statistics, San Diego State University, San Diego, California

Abstract

Current therapeutic approaches to cancer are designed to target molecules that contribute to malignant behavior but leave normal tissues intact. β_1 integrin is a candidate target well known for mediating cell-extracellular matrix (ECM) interactions that influence diverse cellular functions; its aberrant expression has been implicated in breast cancer progression and resistance to cytotoxic therapy. The addition of β_1 integrin inhibitory agents to breast cancer cells at a single-cell stage in a laminin-rich ECM (three-dimensional lrECM) culture was shown to down-modulate β_1 integrin signaling, resulting in malignant reversion. To investigate β_1 integrin as a therapeutic target, we modified the three-dimensional lrECM protocol to approximate the clinical situation: before treatment, we allowed nonmalignant cells to form organized acinar structures and malignant cells to form tumor-like colonies. We then tested the ability of β_1 integrin inhibitory antibody, AIIB2, to inhibit tumor cell growth in several breast cancer cell lines (T4-2, MDA-MB-231, BT474, SKBR3, and MCF-7) and one nonmalignant cell line (S-1). We show that β_1 integrin inhibition resulted in a significant loss of cancer cells, associated with a decrease in proliferation and increase in apoptosis, and a global change in the composition of residual colonies. In contrast, nonmalignant cells that formed tissue-like structures remained resistant. Moreover, these cancer cell–specific antiproliferative and proapoptotic effects were confirmed *in vivo* with no discernible toxicity to animals. Our findings indicate that β_1 integrin is a promising therapeutic target, and that the three-dimensional lrECM culture assay can be used to effectively distinguish malignant and normal tissue response to therapy.
(Cancer Res 2006; 66(3): 1526-35)

Introduction

Development of monoclonal antibody therapies designed to target aberrant cell surface signaling receptors, such as HER-2 and epidermal growth factor receptor (EGFR), have shown great promise in cancer therapy (1, 2). One other class of cell surface receptors that is critical in mediating cell-extracellular matrix (ECM) interactions is β_1 integrin, a major contributor for growth factor receptor signaling. β_1 integrins belong to a family of heterodimeric transmembrane receptors that transmit biomechanical cues that critically mediate cell-ECM interactions (reviewed in ref. 3). β_1 integrin is aberrantly expressed in human breast carcinomas and has been shown to play a central role in growth, apoptosis, invasion, and metastasis (4–8). In addition to its role in cancer progression, an emerging body of evidence indicates that β_1 integrin signaling plays a significant role in mediating resistance to cytotoxic chemotherapies by enhancing cell survival in hematologic malignancies, lung, and breast cancers (9–12). Inhibition of β_1 integrin has also been shown to abrogate the formation of metastasis in gastric and breast cancer models (13–15). Thus, several aspects of β_1 integrin signaling point to it as a multifaceted target for breast cancer therapy.

Using a three-dimensional lrECM cell culture model, which emulates a more physiologically relevant microenvironment (16), we showed previously that down-modulation of β_1 integrin and growth factor signaling pathways resulted in reversion of the malignant phenotype (17), leading to growth arrest and reformation of tissue polarity (18). In addition, β_1 integrin and growth factor signaling were found to be integrated in the context of the three-dimensional lrECM but not on tissue culture plastic (18, 19).

We reasoned that a modified version of this culture model could provide an accurate surrogate for testing therapies for human breast cancer cells and tumors. We developed the modified three-dimensional lrECM assay and show that inhibition of β_1 integrin results not only in antiproliferative and proapoptotic effects in malignant cell lines in three-dimensional cultures, but that these results were recapitulated also *in vivo*. β_1 integrin inhibition preferentially affected malignant cells both in culture and *in vivo*; the nonmalignant acini and normal tissues were not affected, and remarkably, there was little or no toxicity to the animals.

Materials and Methods

Cell culture. HMT-3522-S1 (S-1) mammary epithelial cells were originally derived from a woman with nonmalignant fibrocystic breast disease (20) and cultured in H14 medium as previously described (17). S-1 cells were propagated on plastic in medium containing 10 ng/mL EGF, and T4-2 cells were grown on collagen type I–coated flasks in the absence of EGF (17). Human breast cancer cell lines MCF-7 and MDA-MB-231 were obtained from the American Type Culture Collection (Manassas, VA), and SKBR-3 and BT474 were a gift from Dr. Joe Gray (University of California in San Francisco, UCSF). Three-dimensional cultures were plated with cells trypsinized from monolayer cultures and plated on top of commercially available matrix produced from Englebreth-Holm-Swarm tumors (Matrigel, Collaborative Research, Waltham, MA). Cell lines were maintained in media described above, conditioned with 5% Matrigel. This assay is distinct from

Note: Supplementary data for this article are available at Cancer Research Online (http://cancerres.aacrjournals.org/).

Requests for reprints: Catherine Park, University of California in San Francisco/Mt. Zion Cancer Center, 1600 Divisadero Street H1031, San Francisco, CA 94143-1708. Phone: 415-353-7186; Fax: 415-353-9883; E-mail: park@radonc17.ucsf.edu.

doi:10.1158/0008-5472.CAN-05-3071

previously published reversion assays that were done with cells completely embedded within Matrigel (17). Cells were plated on day 0. For S-1 cultures, AIIB2 was added on day 6 of culture, after acinar formation had occurred. For malignant cell lines, AIIB2 was added on day 4 of culture, after cells had undergone several population doublings. All cultures were analyzed after 3 days of AIIB2 treatment.

β_1 integrin and HER-2 inhibitory antibodies. AIIB2, a β_1 integrin function-blocking antibody (originally a gift from C. Damsky, UCSF) was isolated and prepared from a hybridoma cell line (Sierra Biosources, Milipitas, CA). AIIB2 is a rat monoclonal IgG1 that was originally isolated from a human choriocarcinoma hybridoma that specifically binds β_1 integrin extracellular domain (21–23). Experiments using $F(ab')_2$ fragments of enzyme-digested AIIB2 indicated that the epitope-binding portion of the antibody was active and resulted in down-modulation of β_1 integrin–mediated signaling (17, 19). AIIB2 was added to culture medium on alternate days. Herceptin is a humanized monoclonal antibody against the erbB2 or HER-2 receptor (24) that was used (20 μg/mL) to treat SKBR3 cells on day 6. Control cultures for all experiments were treated with the same concentration of nonspecific IgG.

Immunofluorescence. Cells from three-dimensional cultures were fixed onto a glass slide using 4% paraformaldehyde or methanol/acetone. Nonspecific sites were blocked with 0.5% casein/PBS solution for 1 hour at room temperature. Primary β_1 integrin monoclonal rat anti-mouse antibody (PharMingen, San Diego, CA; 1:100) was diluted in blocking buffer and was applied for 1 hour at room temperature in a humidified chamber. Slides were washed in PBS containing 0.1% bovine serum albumin, before incubating in secondary antibody conjugated to FITC (Molecular Probes, Eugene, OR) for 1 hour in a dark humidified chamber at room temperature. The slides were then washed and counterstained with 4′,6-diamidino-2-phenylindole before mounting with Vectashield mounting medium (Vector Laboratories, Burlingame, CA).

Confocal microscopy. Confocal images were acquired by using a Zeiss LSM 410 inverted laser scanning confocal microscope equipped with an external argon/krypton laser. Using a Zeiss Fluor ×40 (1.3 numerical aperture) objective, images were captured at the colony midsection. Relative immunofluorescence intensity of images was standardized by comparing only cultures that were processed identically and stained in the same experiment.

Western immunoblot. Cells propagated in three-dimensional lrECM were first treated with ice-cold PBS/EDTA [0.01 mol/L sodium phosphate (pH 7.2) containing 138 mmol/L sodium chloride and 5 mmol/L EDTA] to isolate the cells and then lysed in radioimmunoprecipitation assay buffer as previously described (17). Equal amounts of protein were loaded onto reducing SDS gels. After transfer onto nitrocellulose membrane (Invitrogen, Carlsbad, CA), blots were blocked with 5% nonfat milk and probed. Primary antibodies used include β_1 integrin, clone 18 (1:1,000), phospho-FAK, clone 14 (1:1,000; BD Transduction Laboratories, Lexintgon, KY); phospho-β_1 integrin (1:1,000; Biosource, Camarillo, CA); β-actin, clone AC-15 (1:5,000; Sigma, St. Louis, MO). Blots were washed, incubated with secondary antibody, and exposed to X-ray film.

Fluorescence-activated cell sorting analysis. Cells were propagated on tissue culture plastic and harvested using 0.25% trypsin. After resuspending in 1 mL DMEM/F-12 media with trypsin inhibitor, cells were spun down and washed in 1× PBS, 5% fetal bovine serum, and 0.1% sodium azide on ice. Cells were incubated with primary antibody (AIIB2, 1:10) at 4°C for 30 minutes to 1 hour, washed, and incubated with a fluorescein-conjugated IgG secondary antibody (1:100) for 30 minutes. After washing, 1 mL of 1% paraformaldehyde solution was added to the pellet and suspended immediately. Cells were analyzed using a Beckman-Coulter EPICS XL-MCL Analyzer. System II Data Acquisition and Display software, version 2.0 was used for data analysis.

Apoptosis and proliferation assays. Apoptosis was assayed in cell culture using a commercially available kit (In Situ Cell Death Detection kit, fluorescein; Roche, Nutley, NJ) designed to detect terminal deoxynucleotidyl transferase (TdT)–mediated nick end labeling (TUNEL). Cells were fixed in 4% paraformaldehyde and permeabilized in cold 0.1% Triton X-100 in 0.1% sodium citrate. After washing in PBS, cells were incubated in TUNEL reaction mixture at 37°C for 60 minutes, washed, and mounted. Proliferation was detected by indirect immunofluorescence of Ki-67 nuclear antigen. Cells were fixed in methanol/acetone and blocked using 10% goat serum, then incubated in primary rabbit antibody against Ki-67, clone MIB-1 (1:200; Novocastra Laboratories, Norwell, MA) for 1 hour and washed before FITC-conjugated anti-rabbit secondary antibody (The Jackson Laboratory, Bar Harbor, ME) was applied. Nuclei were counterstained with DAPI.

For assay of apoptosis in paraffin-embedded tissues, Apoptag In Situ Apoptosis Detection kit (Intergen, Burlington, MA) was used to detect TUNEL reaction. Paraffin-embedded xenograft tumors were sectioned at 5- to 10-μm-thick sections. Sections were deparaffinized and rehydrated using xylene and ethanol washes. Tissues were then treated with proteinase K at room temperature, washed, and quenched using 3% hydrogen peroxide. Buffer solution was applied, and sections were incubated in TdT enzyme at 37°C for 1 hour. Stop/wash buffer was used before anti-digoxigenin peroxidase conjugate was applied. Proliferation was assayed in paraffin-embedded tissues using indirect immunohistochemistry. Sections were deparaffinized as above and blocked using 10% normal horse serum, then incubated with mouse monoclonal antibody against Ki-67 (Oncogene, San Diego, CA) overnight at 4°C, and washed in PBS. They were then serially incubated with biotinylated anti-mouse antibody, and steptavidin-horseradish peroxidase and 3,3′-diaminobenzidine (DAPI) medium. After counterstaining with hematoxylin, sections were dehydrated in serial concentrated ethanol and xylene and mounted. Cells were scored by counting the total number of nuclei in five high-power microscopic fields (×40) using a ×10 objective, or a minimum of 200 nuclei per tumor section.

Tumor growth and toxicity assessment *in vivo*. Female $nu^{-/-}$ mice were obtained from Charles River (Wilmington, MA) or Taconic (Germantown, NY) and housed five per cage with chow and water *ad libitum* in a controlled animal barrier. Animals were injected s.c. with 5 to 10×10^6 T4-2 cells or 10^7 MCF-7 cells into the upper back posterior to the right front limb. Estradiol pellets were inserted s.c. above the tail for animals bearing MCF-7 xenografts. AIIB2 antibody or nonspecific rat IgG was injected into the i.p. cavity biweekly beginning on day 4 or day 28 after cell implantation. Tumor dimensions (width, height, and depth) were measured biweekly. At the time of sacrifice, animals were euthanized, and tumors were harvested and either immediately frozen in ornithine carbamyl transferase or fixed in formalin. Serum was collected using cardiac puncture techniques.

Animals were monitored for evidence of toxicity by measuring weight, assessing overall activity, and necropsy. Additional toxicity studies were done using β_1 integrin inhibitory antibody, clone Ha 2/5 (PharMingen), which specifically recognizes murine β_1 integrin. Antibody was administered at doses of 1 to 20 mg/kg biweekly over 4 weeks. All experimental procedures were followed according to the UCSF, and LBNL Animal Welfare Committees approved policies and guidelines.

Statistical analysis. For each dose of AIIB2 or control IgG in culture, pairwise differences in Ki-67 or TUNEL were tested among the six cell lines using Student's *t* test (25). Multivariate ANOVA was used for analysis of tumor volume at each time point. For each dose of AIIB2 or control IgG *in vivo*, pairwise Student's *t* test or χ^2 comparison was used to analyze differences between TUNEL and Ki-67 expression. MINITAB (Minitab, Inc., State College, PA) statistical software was used for all calculations.

Results

β_1 integrin inhibition results in cytostasis and apoptosis in breast cancer cell colonies treated in three-dimensional cultures. We showed previously that down-modulation of β_1 integrin downstream signaling pathways in *single* cancer cells embedded within three-dimensional lrECM was associated with phenotypic reversion, exemplified by growth arrest and acinar differentiation (17, 26), whereas *single* nonmalignant mammary epithelial cells underwent apoptosis (27). We sought to explore whether there is a role for β_1 integrin as a molecular target in

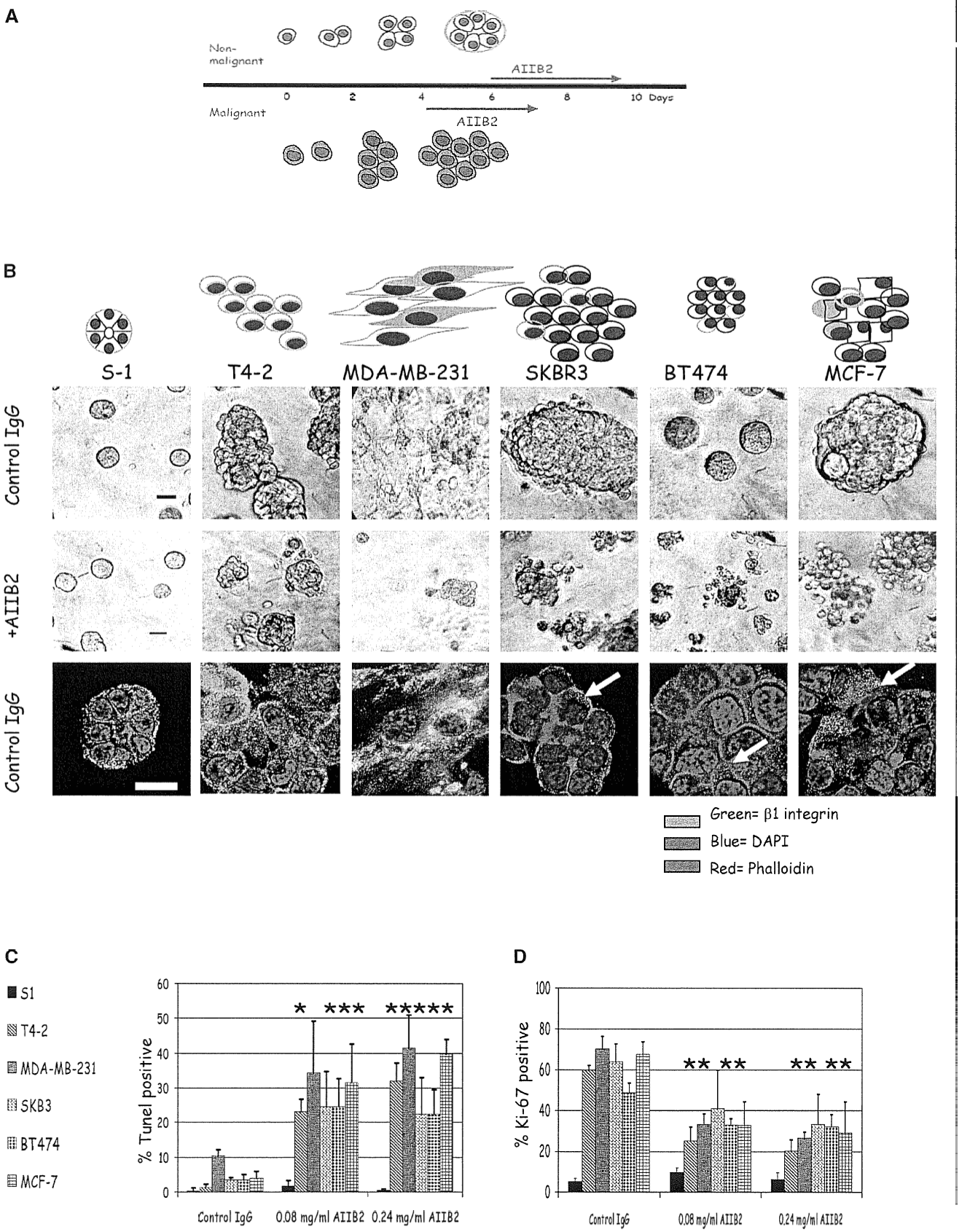
A
Non-malignant
AIIB2
0
2
4
6
8
10 Days
Malignant
AIIB2
B
S-1
T4-2
MDA-MB-231
SKBR3
BT474
MCF-7
Control IgG
+AIIB2
Control IgG
Green= β1 integrin
Blue= DAPI
Red= Phalloidin
C
S1
T4-2
MDA-MB-231
SKB3
BT474
MCF-7
% Tunel positive
60
50
40
30
20
10
0
* *** *****
Control IgG
0.08 mg/ml AIIB2
0.24 mg/ml AIIB2
D
% Ki-67 positive
100
80
60
40
20
0
** ** ** **
Control IgG
0.08 mg/ml AIIB2
0.24 mg/ml AIIB2

breast cancer, which relies on the differential response between normal and malignant tissues. In patients, tumors are commonly discovered *after* a multicellular three-dimensional tumor has already been formed, and normal cells are found in an organized three-dimensional context. We reasoned that this scenario could be emulated also in the three-dimensional lrECM assay. In addition, we wanted to know whether we could then distinguish between the response of normal and malignant structures. Accordingly, we modified the three-dimensional lrECM assay to test these concerns.

When cultured on top of three-dimensional lrECM gels with 5% Matrigel conditioned media, nonmalignant breast cells undergo morphogenesis and, after 6 days, form acini with polarized cells oriented around a central lumen with a well organized basement membrane, recapitulating normal acinar structures found *in vivo* (Fig. 1*A*; for review, see ref. 28). In contrast, all malignant breast cell lines tested (T4-2, MDA-MB-231, SKBR3, BT474, and MCF-7) continued to proliferate and formed disorganized tumor colonies (Fig. 1*A*). Our previous studies have shown that β_1 integrin inhibitory monoclonal antibody, AIIB2, or its $F(ab')_2$ fragments applied to single cells were capable of down-modulating β_1 integrin signaling pathways (17, 19). In the present studies, breast cancer cell lines were propagated in three-dimensional lrECM until colonies were formed (4 days) and were then treated with AIIB2 at doses ranging from 0.08 to 0.24 mg/mL, or with isotype-matched nonspecific rat IgG1 as control (Fig. 1*B*). Using confocal microscopy, we show that β_1 integrin was appropriately localized to the basolateral surfaces of the S-1 cells within the acini, as is the case *in vivo*. In contrast, it was diffusely distributed around the surfaces of each cell within T4-2 and MDA-MB-231 colonies in three-dimensional lrECM, and little expression was seen on three of the other cell lines (Fig. 1*B*).

In assays starting from single cells, AIIB2 concentrations of 0.10 to 0.16 mg/mL were sufficient to induce reversion (17, 19). In the current procedure, colonies were analyzed for percentage of proliferating cells using Ki-67 nuclear antigen and for apoptosis by TUNEL assay. After 3 days of treatment, all but one of the malignant cell lines showed a significant proportional decrease in the percentage of proliferating cells (46-54% of Ki-67 expressing cells at 0.08 mg/mL AIIB2 and 0.24 mg/mL AIIB2, respectively; $P < 0.02$, Student's t test for any AIIB2 dose compared with controls for T4-2, MDA-MB-231, BT-474, and MCF-7; Fig. 1*C*). The only exception among the five malignant cell lines was SKBR3, which did not show a significant decrease in the percentage of Ki-67–positive cells with AIIB2 treatment. Apoptosis was assayed simultaneously: there was a dramatic increase in TUNEL-positive nuclei for all malignant cell lines (85-88% at 0.08 mg/mL AIIB2 and 0.24 mg/mL AIIB2, respectively; Fig. 1*D*; $n = 3$). For the MDA-MB-231 cell line, the higher dose of AIIB2 was associated with a statistically significant increase in TUNEL-positive nuclei, whereas the P approached significance for the lower dose (hence the absence of the *).

In contrast, the nonmalignant cell line S-1 formed acinar structures when cultured on top of three-dimensional lrECM for 6 days and, unlike colonies made of malignant cells, did not undergo increased apoptosis or cytostasis upon addition of AIIB2 regardless of the dose used (Fig. 1*C* and *D*). Similar results were obtained for S-1 cells treated at day 4 (data not shown). In addition, there was no significant change in the distribution of the size or number of total colonies (data not shown). Previous studies have shown that AIIB2 applied to single S-1 cells induce apoptosis (27); however, in the present study, we show that when S-1 cells are in the context of organized structures, they are resistant to apoptosis. This indicated that the signaling context of β_1 integrin is critical to response to AIIB2 treatment: nonmalignant mammary epithelial cells with intact cell-cell and cell-ECM interactions were resistant to the inhibitor. These results confirm and extend studies of conventional apoptotic and chemotherapeutic agents tested previously in the single-cell assay in three-dimensional lrECM (29).

Coexpression of total β1 integrin, phosphorylated β_1 integrin, and phosphorylated ^{397}FAK among breast cell lines cultured in three-dimensional lrECM. β_1 Integrin expression detected by immunofluorescence was characterized by basolateral localization in nonmalignant S-1 acinar structures and disorganized and aberrant expression in the malignant cell lines. To further characterize β_1 integrin expression, we analyzed cell lysates for total β_1 integrin levels using Western immunoblotting. Total β_1 integrin expression corresponded to that detected using immunofluorescence; three cell lines (S-1, T4-2, and MDA-MB-231) showed relatively higher levels of β_1 integrin compared with SKBR3, BT474, and MCF-7 (Fig. 2*A*). In addition, fluorescence-activated cell sorting (FACS) analysis confirmed the surface expression of β_1 integrin reflected that detected using immunofluorescence and Western blot (Fig. 2*B*). We concluded that β_1 integrin expression was variable, and response to β_1 integrin inhibitory antibody did not seem to correlate with total levels of β_1 integrin expression in individual cell lines.

We reasoned that signaling proteins that are critical in β_1 integrin signaling, such as phosphorylation of β_1 integrin cytoplasmic tail (30), or focal adhesion kinase (FAK; refs. 31, 32), may correlate with response to AIIB2 treatment. To test this, protein lysates from the six cell lines propagated in three-dimensional lrECM were used to detect relative coexpression of β_1 integrin, phosphorylated β_1 integrin (p-β_1 integrin), and phosphorylated ^{397}FAK (p-^{397}FAK). We found that p-β_1 integrin levels were relatively lower in S-1, T4-2, and MDA-MB-231 cells compared with SKBR3, BT474, and MCF-7 cell lines, which inversely correlated with total β_1 integrin levels (Fig. 2*A*). p-^{397}FAK levels did not seem to correlate with total β_1 integrin or p-β_1 integrin levels. Interestingly, p-^{397}FAK levels were lowest in SKBR3 cells, which were refractory to AIIB2-induced cytostasis.

SKBR3 colonies respond to a combination of AIIB2 and Herceptin. The SKBR3 cell line overexpresses erbB2 (HER-2), a

Figure 1. Morphology and response of breast cell lines to β_1 integrin inhibition in three-dimensional lrECM. Five malignant breast cell lines (T4-2, MDA-MB-231, SKBR3, BT474, and MCF-7) and one nonmalignant breast cell line (S-1) were propagated in three-dimensional lrECM and treated with β_1 integrin inhibitory antibody, AIIB2, after colonies were formed. *A,* schema of the three-dimensional lrECM assay used in this study. *B, top* and *middle,* phase-contrast micrographs of cultured colonies before and after antibody treatment, respectively. Bar, 20 μm. *Bottom,* confocal midsections of β_1 integrin immunofluorescence (▭) of colonies cultured in three-dimensional lrECM. Phalloidin was used to stain actin filaments (▭), and DAPI was used to stain individual nuclei (▭). Bar, 13 μm for all cell lines shown. *C,* whereas there were no significant changes in Ki-67 or TUNEL expressing cells among nonmalignant S-1 cells after β_1 integrin inhibition, malignant cell lines, except SKBR3, had a significant decrease in Ki-67 expressing cells and a significant increase in TUNEL-positive cells after antibody treatment. *Columns,* mean ($n = 3$); *bars,* SE. $P < 0.05$, t test.

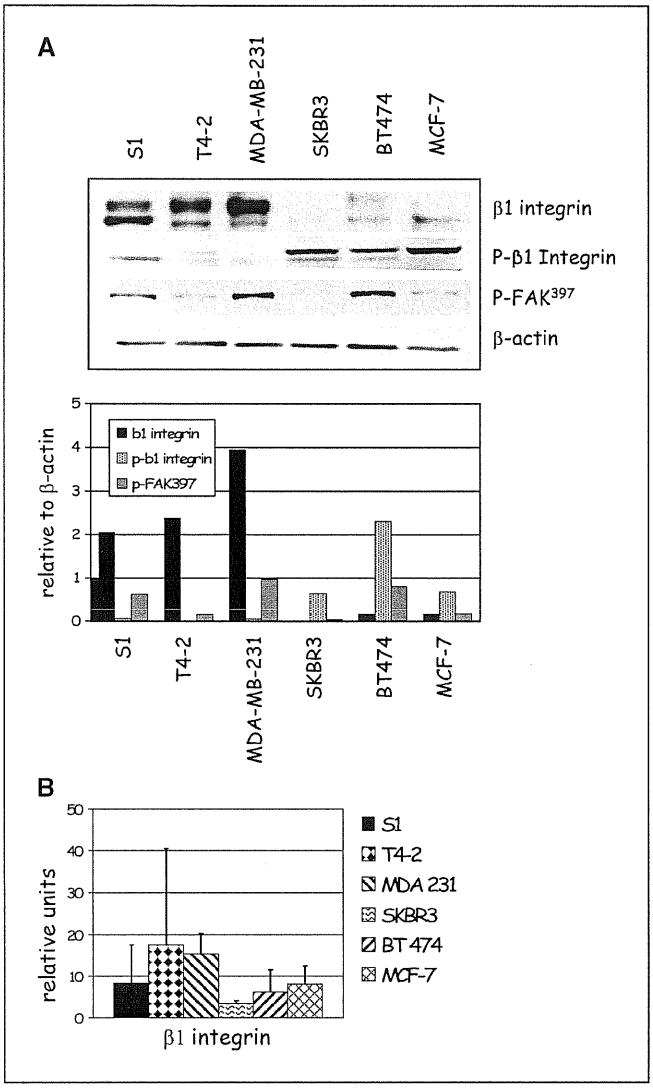

Figure 2. β_1 Integrin, p-β_1 integrin, and p-^{397}FAK are expressed at different levels in breast cell lines in three dimensions. Lysates from five breast cancer cell lines (T4-2, MDA-MB-231, SKBR3, BT474, and MCF-7) and one nonmalignant cell line (S-1) in three-dimensional lrECM were probed by Western immunoblotting for total and p-β_1 integrin and p-^{397}FAK and for surface β_1 integrin expression by FACS analysis. *A,* total β_1 integrin levels are relatively high in S-1, T4-2, and MDA-MB-231 cells compared with SKBR3, BT474, and MCF7 cells. Conversely, p-β_1 integrin levels are relatively low in S-1, T4-2, and MDA-MB-231 cells compared with SKBR3, BT474, and MCF7 cells. Expression of p-^{397}FAK is expressed among all cell lines except SKBR3, where it is undetectable by Western blots. *B,* surface expression of β_1 integrin by FACS analysis corresponds to that seen by immunofluorescence (Fig. 1*B*) and Western blots (Fig. 1*A*).

member of the EGF family of growth factor receptors. β_1 integrin has been shown to cooperate with other members of the EGF family, such as erbB1 (19); however, the relationship between HER-2 and β_1 integrin signaling is not well understood. We reasoned that HER-2 signaling was one factor that could contribute to the decreased cytostatic response of SKBR3 cells treated with AIIB2. Herceptin is a monoclonal antibody directed against HER-2 and has a significant role in treatment of patients with HER-2 overexpressing breast cancer (33). Therefore, we tested the effect of Herceptin and AIIB2 in combination in SKBR3 cells. Compared with colonies treated with nonspecific control IgG, SKBR3 colonies treated with AIIB2 or Herceptin alone showed a proportional decrease in Ki-67–positive cells (44.8% for AIIB2 and 39.1% for Herceptin). However, colonies that were treated with both AIIB2 and Herceptin had an augmented proportional decrease in Ki-67–positive cells (68.8%; $P < 0.05$, χ^2; Supplementary Fig. S1).

β_1 integrin inhibition preferentially affects larger tumor masses with a global redistribution in colony size and morphology. To determine the effect of treatment on the colony population as a whole, we counted the total number of cells and then scored for individual colonies by size. Using T4-2 cells as a prototype, we found that β_1 integrin inhibition resulted in a significant decrease in total cell number (Fig. 3*A*, mean ± SE; $P < 0.05$, χ^2). To further examine how the treatment influenced the global composition of colonies in the population, we counted the number of cells within each colony after 3 days of treatment. The mean colony size decreased from 12 to 6 cells with treatment reflected by the distribution of the size of colonies (Fig. 3*B*, mean ±

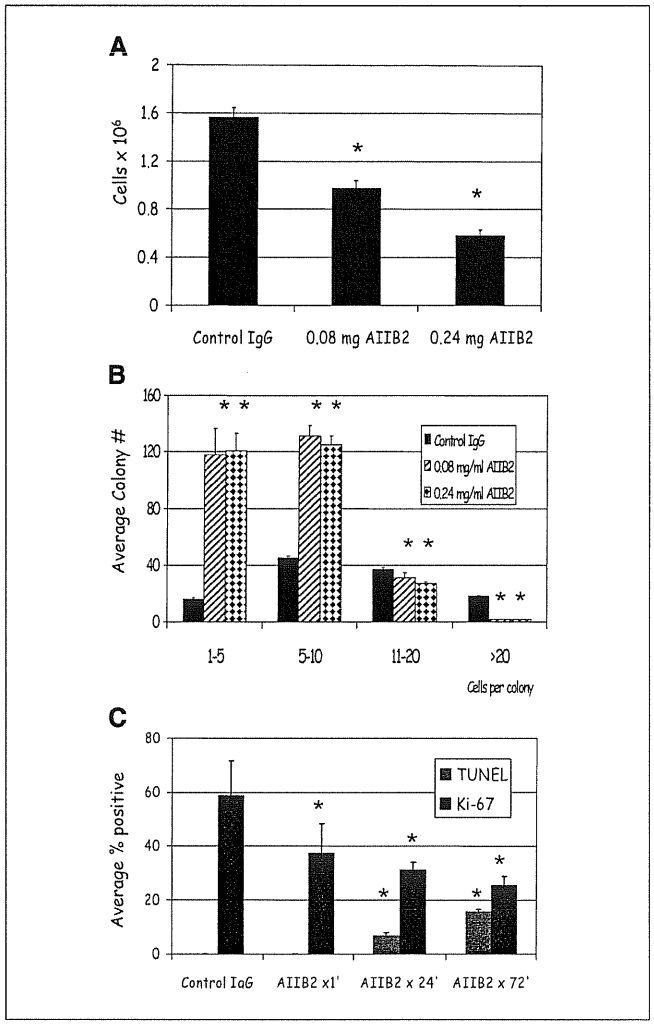

Figure 3. AIIB2 reduces both total cell number and average colony size in malignant cell lines. *A,* average number of T4-2 cells after 3 days of treatment with AIIB2. *Columns,* mean; *bars,* SE. $P < 0.05$, χ^2. *B,* histogram showing the average colony size decreased with AIIB2 compared with controls. *Columns,* mean; *bars,* SE. $P < 0.05$, *t* test. *C,* percentage of Ki-67 and TUNEL expressing nuclei among T4-2 cells 1, 24, and 72 hours after addition of AIIB2 to cultures. *Columns,* mean; *bars,* SE. $P < 0.05$, *t* test.

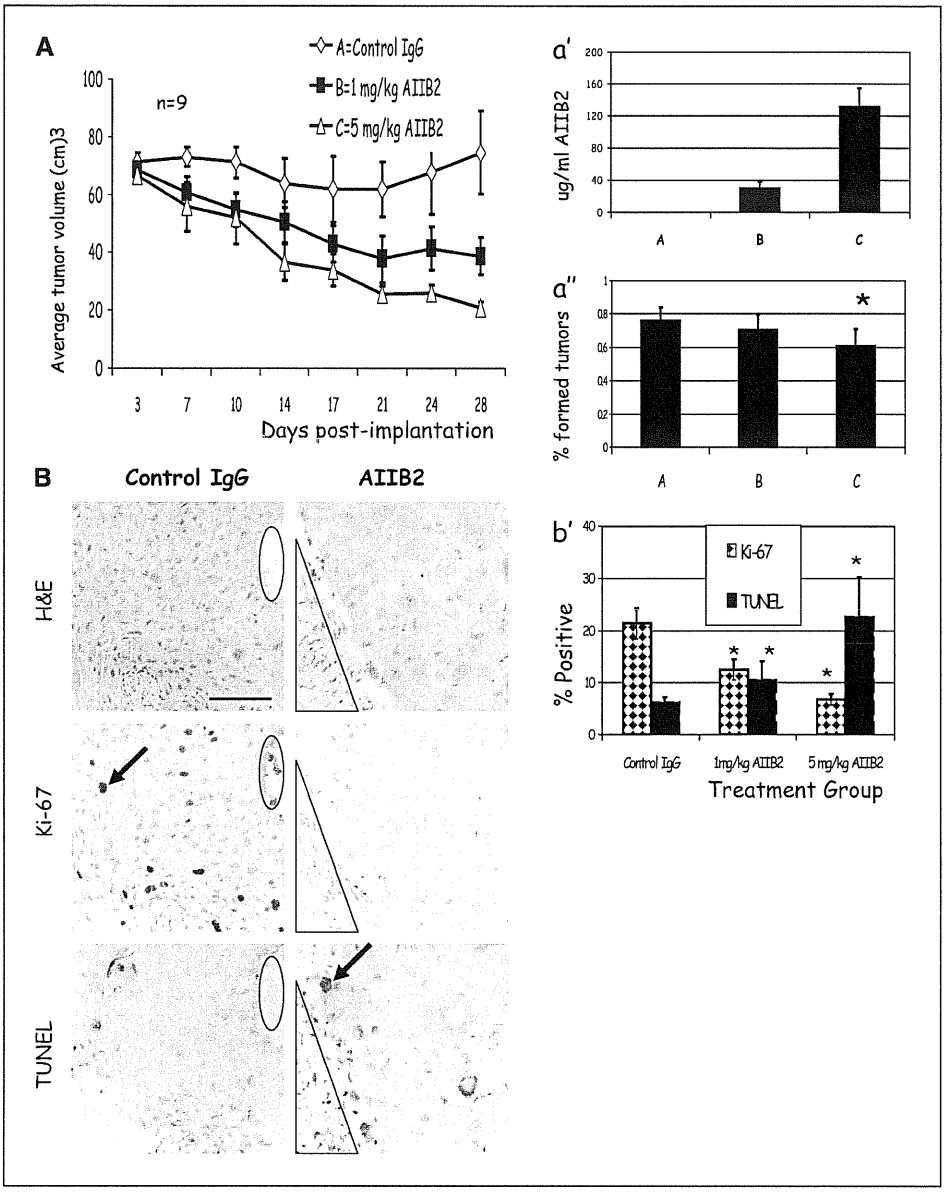

Figure 4. AIIB2 suppresses tumor growth *in vivo* by enhancing apoptosis and decreasing proliferation. *A*, mean tumor volumes among animals that received 1 mg/kg AIIB2 (■) or 5 mg/kg AIIB2 (△) were significantly smaller than control animals (♦). *Points*, mean (n = 9); *bars*, SE. *A'*, average serum concentration (μg/mL) of AIIB2 at the time of sacrifice was significantly higher in animals receiving AIIB2 compared with control vehicle. *Columns*, mean; *bars*, SD. *A''*, average number of animals in each treatment group that had histologic evidence of tumor at the time of sacrifice was significantly lower among treated animals compared to controls. *Columns*, mean for three separate experiments; *bars*, SE. *, $P < 0.03$, χ^2. *B*, micrographs of serial sections of tumors that were scored for apoptosis by the presence of TUNEL-positive nuclei and for proliferation by the presence of Ki-67 nuclear antigen. *Black ovals* and *triangles*, coregistered regions in serial sections; *arrows*, examples of positive staining. *B'*, with AIIB2 treatment, the average number of TUNEL nuclei increased, and the number of Ki-67–positive nuclei decreased. *Columns*, mean; *bars*, SE. *, $P < 0.05$, χ^2. Bar, 247 μm.

SE; $P < 0.05$, t test). Similar results were seen for all other cancer cell lines (data not shown). To investigate the time course and mechanism of these changes, we counted the average number of Ki-67– and TUNEL-positive nuclei in the T4-2 cultures as a function of time after addition of AIIB2 (Fig. 3*C*, mean ± SE; $P < 0.05$, t test). The number of proliferating cells decreased dramatically even within 1 hour after addition of AIIB2, indicating an immediate growth arrest. The percentage of TUNEL-positive nuclei increased from 24 to 72 hours.

Treatment with AIIB2 results in decreased tumor formation, increased apoptosis, and cytostasis *in vivo*. We have shown previously that breast cancer cells that have been pretreated with β_1 integrin inhibitors before injection into nude mice have decreased ability to form tumors *in vivo* (17, 26). To determine the efficacy and optimal dose of AIIB2 that effectively inhibits tumor formation *in vivo*, we tested the ability of AIIB2 to inhibit untreated T4-2 cells to form tumors in adult female $nu^{-/-}$ mice. Animals were implanted with 5 to 10 × 10^6 T4-2 cells or 10^7 MCF-7 cells either s.c. or into the mammary fat pad on day 0. Three groups of mice (n = 9) received biweekly i.p. injections of (*a*) isotype-matched nonspecific rat IgG1, (*b*) 1 mg/kg AIIB2, or (*c*) 5 mg/kg AIIB2 in a blinded fashion beginning on day 4. Tumors were measured biweekly, and volume was estimated by multiplying width × length × depth. Compared with tumors propagated in animals that received control IgG, there was a significant dose-dependent decrease in the volume of treated tumors (Fig. 4*A*) and in the number of animals harboring tumors (Fig. 4*A'*; $P < 0.03$, χ^2). After 4 weeks, animals were sacrificed, serum was analyzed for AIIB2 levels, and tumors were analyzed for histology. Compared with controls, treated animals had a dose-dependent level of AIIB2 detectable in serum samples (Fig. 4*A''*, mean ± SE; $P < 0.05$, χ^2). Representative micrographs of the same coregistered region of a tumor stained with H&E, Ki-67, and TUNEL are shown (Fig. 4*B*).

Sections from each tumor were evaluated for apoptosis by TUNEL assay and proliferation by Ki-67 (Fig. 4*B'*). Compared with controls, treated tumors had significantly decreased percentage of Ki-67–positive cells and a significantly increased level of TUNEL-positive nuclei (mean ± SE; $P < 0.05$, χ^2). In addition, tumors treated with 5 mg/kg AIIB2 had significantly higher percentage of caspase-3–positive cells (11 ± 2%) compared with controls (3.13 ± 0.7%; $P < 0.05$, χ^2). Similar results were obtained for MCF-7 xenografts treated with AIIB2 *in vivo* (data not shown).

AIIB2 is effective against established tumors *in vivo*. To further evaluate the efficacy of AIIB2 *in vivo*, we allowed MCF-7 cells to continue to grow for ~4 weeks and then randomized animals to receive nonspecific rat IgG1, 1 mg/kg AIIB2, or 5 mg/kg AIIB2 for four additional weeks. Compared with controls, treated animals had significantly less tumor growth (Fig. 5*A*). In addition, histologic analysis showed that treated tumors had significantly fewer Ki-67–positive cells compared with controls (Fig. 5*B*, mean ± SE; $P < 0.001$, χ^2) and significantly decreased TUNEL-positive nuclei (Fig. 5*B*, mean ± SE; $P < 0.01$, χ^2). Similar results were found for T4-2 xenografts treated *in vivo* (data not shown).

There is no discernible toxicity with β_1 integrin inhibition *in vivo*. Animals were monitored for any signs of toxicity by measuring weekly weight and assessing activity and general appearance. There was no difference in animal weight between the treated or control groups (Fig. 5*C*), and no discernible toxicity among any groups, up to AIIB2 doses of 20 mg/kg administered biweekly over 4 weeks (data not shown).

Although AIIB2 seems to cross react with murine β_1 integrin,[6] we sought to further evaluate the potential toxicity of broad β_1 integrin inhibition *in vivo*. Therefore, we used clone Ha2/5, a β_1 integrin function-blocking antibody that recognizes murine β_1 integrin. Adult female $nu^{-/-}$ mice were treated with serially increasing doses of antibody from 1 to 20 mg/kg over 4 weeks via biweekly i.p. injection. There were no differences in body weight, activity, overall appearance, or examination at necropsy among animals receiving antibody compared with controls, and no evidence of toxicity among any groups (data not shown).

Discussion

Recent advances in cancer therapy have taken advantage of the aberrant receptors in tumor cells to inhibit growth and enhance the efficacy of conventional cytotoxic treatments (2). β_1 Integrin belongs to a class of cell surface receptors that not only facilitates growth factor receptor signaling but also plays diverse roles in mediating multiple aspects of malignant cell behavior. Indeed, expression of β_1 integrin was shown recently to be necessary for formation of mammary tumors in engineered murine models (4). In addition, β_1 integrin has been shown to enhance survival by mediating resistance to cytotoxic treatment in several cancers (9, 34). The success of any therapy depends on its ability to distinguish between malignant and normal tissues or the therapeutic index. Taking advantage of the modified three-dimensional lrECM culture assay, we show that β_1 integrin inhibitory monoclonal antibody effectively distinguishes between normal and malignant tissue structures. Treatment of malignant

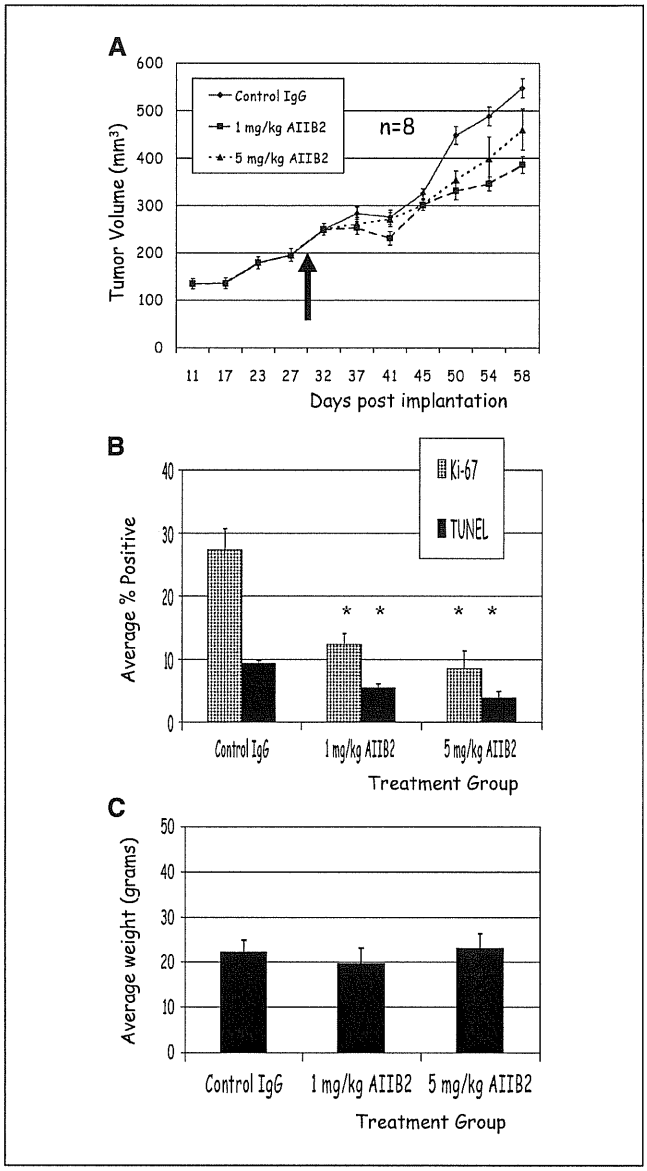

Figure 5. AIIB2 effectively induces cytostasis in established MCF-7 tumors *in vivo* with no toxicity. *A*, animals were randomized to receive treatment or control IgG 4 weeks after MCF-7 cell implantation (*arrow*, time of randomization at day 30). Mean tumor volumes for animals receiving 1 mg/kg AIIB2 (■) and 5 mg/kg AIIB2 (△) and nonspecific rat IgG1 (◆). *Points*, mean ($n = 8$); *bars*, SE. *B*, compared with controls, tumors from animals that received AIIB2 treatment had significantly fewer Ki-67–positive nuclei and fewer TUNEL-positive nuclei. *Columns*, mean; *bars*, SE. *, $P < 0.001$, χ^2. *C*, average weight of control animals, and animals that received AIIB2 treatment were not significantly different at any biweekly time point measured throughout the experiment (data not shown) and at the end of the experiment. *Columns*, mean; *bars*, SE.

colonies with AIIB2 resulted in a dramatic loss in total cell number with a concomitant decrease in proliferation and increase in apoptosis. In addition, there was a global redistribution in the malignant colony size and morphology, reflected by a decrease in mean colony size. In contrast, nonmalignant epithelial cells that were capable of forming organized and polar structures with appropriate cell-ECM interactions remained intact and were resistant to β_1 integrin inhibition. *In vivo*, AIIB2 treatment inhibited tumor growth with an associated decrease in proliferation and increase in cell death in early

[6] Unpublished data.

treated tumors and a decrease in proliferation in treatment of established tumors, with no measurable toxicity to the host. Overall, these results indicate that β_1 integrin inhibition is a potentially viable therapeutic approach in the treatment of breast cancer.

The use of three-dimensional cultures provides a physiologically relevant context in which to emulate cells *in vivo* (35, 36) and has been used previously to investigate novel mechanisms of drug resistance in cancer cells that are demonstrable specifically only in a three-dimensional setting when the appropriate basement membrane molecules are present (37, 38). To model the differences between normal and malignant tissues, we took advantage of the ability of a nonmalignant cell line, HMT-3522-S-1, to undergo normal morphogenesis in three-dimensional lrECM, in contrast to malignant cells that continue to form disorganized invasive colonies. This allowed us to examine the effects of β_1 integrin inhibition on the morphology of cancer cell colonies as a population and to distinguish the potential effects on nonmalignant acini. We had shown previously that nonmalignant cells that were treated with β_1 integrin inhibition as single cells were susceptible to apoptosis (27, 39). However, the response of cells within acinar-like tissue structures where β_1 integrin function is relatively intact has not been investigated. We found that in response to 3 days of AIIB2 treatment, all but one malignant cell line in three-dimensional lrECM showed a dramatic loss in total number of cells, coupled with a significant increase in the percentage of apoptotic cells and a significant decrease in the percentage of proliferating cells. In contrast, S-1 cells that formed polar acinar-like structures were entirely resistant to AIIB2. These results indicate that most malignant cells that form colonies in three-dimensional lrECM rely on β_1 integrin signaling for proliferation and survival, whereas in the context of an organized structure, cells were either no longer dependent on β_1 integrin signaling for survival, or that β_1 integrin was not accessible to the antibody.

Further analysis of cell cultures during and after AIIB2 treatment revealed that the largest cancer cell colonies were being affected, resulting in a global change in the morphology and distribution of proliferating cells, reflected in a decrease in mean colony size. This pattern of multiple residual "tumor foci" was seen also *in vivo* (data not shown). The morphologic characteristics of these clones were distinctly different from the untreated tumors, as were features of cell-cell and cell-ECM interactions. These results have implications for clinical treatment. β_1 Integrin has been implicated in mediating resistance to cytotoxic chemotherapies (9, 10), and inhibition of different tumor types may enhance response by abrogating resistance. In addition, ionizing radiation was shown to up-regulate β_1 integrin in cancer cells (40, 41), and our preliminary studies of β_1 integrin inhibition combined with ionizing radiation are promising and may lead to novel strategies for combinatorial therapies to eradicate or further reduce tumor viability *in vivo*.

Several promising biological therapies aimed at signaling pathways have entered clinical trials; however, despite evidence of response to treatment, useful biomarkers have frequently been difficult to validate (1, 42, 43). For example, the current treatment of cancers with EGFR inhibition illustrates the complexity of some molecular targets and the lack of robust predictive markers that would aid in the selection of individuals for treatment (42). The mechanisms that are involved in cytostasis and apoptosis associated with β_1 integrin inhibition in malignant cells are likely to involve interactions between multiple signaling pathways. For example, our previous studies have shown that β_1 integrin signaling pathway integrates and cooperates with the EGFR signaling pathway via mitogen-activated protein kinase and phosphatidylinositol 3-kinase (18, 19). In the present study, we found that β_1 integrin expression on the six breast cell lines used was variable. We probed the cell lines for p-β_1 integrin and p-^{397}FAK to investigate potential markers for β_1 integrin signaling activity. Interestingly, p-β_1 integrin expression was inversely correlated with total β_1 integrin, suggesting that either species is required for β_1 integrin signaling to occur. Although p-^{397}FAK is a requisite protein for focal adhesion formation, its role in β_1 integrin signaling in the context of the cell lines we investigated remains unclear. We recognize that β_1 integrin signaling involves several steps, including activation, heterodimerization, ligand binding, and clustering (44, 45); these functional aspects of β_1 integrin signaling activity may not be reflected by the level of receptor expression and/or status of any single signaling protein alone. The major factor that distinguished the nonmalignant S-1 cells and the malignant cell lines is the organization and polarity of β_1 integrin localization, indicating that the context of signaling may be the most important feature that enhances the therapeutic window. Studies are ongoing to investigate which pathways may be the most robust predictors of response in to β_1 integrin inhibition in the clinical setting.

SKBR3 cells were less responsive to β_1 integrin inhibition compared with other cancer cell lines. This cell line is characteristically devoid of E-cadherin and overexpresses growth factor receptor HER-2 features that could contribute to uncoupling of β_1 integrin signaling and survival (46, 47). Interestingly, BT474 cells, which overexpress HER-2 and estrogen receptor (ER), remain sensitive to AIIB2. In contrast, SKBR3 cells overexpress HER-2 but are ER negative, a phenotype that has implicated growth factor signaling pathways with resistance to tamoxifen (48). Herceptin, a monoclonal antibody against HER-2, has been shown to down-modulate the HER-2 receptor, resulting in cytostasis (24). We found that the addition of Herceptin to AIIB2 in SKBR3 cells in three-dimensional lrECM resulted in a significantly decreased percentage of Ki-67–positive cells compared with cultures treated with AIIB2 alone. These data indicate that an additive cytostatic effect is achieved by using the combination of inhibitory antibodies. Further investigations of the features of SKBR3 that may confer resistance to AIIB2 are warranted and may help identify subsets of tumors that may respond to a combination of β_1 integrin inhibition and Herceptin or hormonal therapy.

We found that β_1 integrin inhibition was effective in both T4-2 and MCF-7 xenografts in nude mice *in vivo*, confirming our results in three-dimensional lrECM. Similar to the response observed in culture, tumor xenografts treated *in vivo* showed decreased proliferation and increased apoptosis compared with controls in the animals that received treatment beginning 4 days after tumor implantation. In animals where the tumors were treated after 4 weeks of implantation, there was a significant decrease in tumor size and proliferation and a decrease in apoptosis in treated animals compared with controls. The decrease in observed TUNEL-positive cells in the larger tumors could be due to the increased amounts of necrosis, an alternate mechanism of cell death, seen in larger tumors (data not shown).

Toxicity studies using AIIB2 and clone Ha2/5 revealed no discernible toxicity in animals, even with 20 mg/kg doses. These

results indicate that β_1 integrin signaling confers growth and survival advantages in cancer cells *in vivo* that can be discriminated from normal β_1 integrin signaling by AIIB2. Other mechanisms also should be considered. For example, immune-mediated secondary effects of the antibody have been shown to play a significant role in antibody-mediated therapies (47). We have previously shown that the $F(ab')_2$ fragments of AIIB2 are active in three-dimensional lrECM assays (17), and others have shown that AIIB2 binds to a region of β_1 integrin extracellular domain between two putative ligand binding sites that are thought to induce a conformational change (48), resulting in down-modulation of signaling. The activity or presence of Fc-directed immune response *in vivo* has not been isolated from the activity of the $F(ab')_2$ region per se. These studies, in addition to humanization of the AIIB2 clone, are necessary next steps towards clinical drug development.

In summary, β_1 integrin inhibition using monoclonal antibody AIIB2 results in cytostasis and apoptosis in malignant breast cancer colonies but not normal tissue structures propagated on top of three-dimensional lrECM gels. The three-dimensional lrECM assay appropriately distinguishes the difference in response between normal structures and malignant colonies and reveals global changes in morphology associated with treatment. In addition, AIIB2 inhibits breast cancer growth *in vivo* by eliciting increased apoptosis and decreased proliferation, with no discernible toxicity to animals. We conclude that β_1 integrin inhibition using monoclonal antibodies is a promising approach to breast cancer treatment, and that the modified three-dimensional lrECM assay and protocol is an appropriate assay for testing differences in malignant and normal cell response to targeted therapeutic agents.

Acknowledgments

Received 8/29/2005; revised 11/12/2005; accepted 11/18/2005.

Grant support: UCSF-REAC; Cooperative Institutional Research Program; NIH P50 Specialized Programs of Research Excellence grant CA CA58207-08 (C. Park); U.S. Department of Energy, Office of Biological and Environmental Research grant DE-AC03-76SF00098 (M.J. Bissell); NIH/National Cancer Institute grants CA64786-09 (M.J. Bissell) and P50 CA112970-01 (J.W. Gray and M.J. Bissell); and U.S. Department of Defense Breast Cancer Research Program's Innovator Award DAMD17-02-1-0438 (M.J. Bissell).

The costs of publication of this article were defrayed in part by the payment of page charges. This article must therefore be hereby marked *advertisement* in accordance with 18 U.S.C. Section 1734 solely to indicate this fact.

We thank Donghui Wang and Evelyn Yao for expert technical assistance.

References

1. Mendelsohn J, Baselga J. The EGF receptor family as targets for cancer therapy. Oncogene 2000;19:6550–65.
2. Slamon DJ, Leyland-Jones B, Shak S, et al. Use of chemotherapy plus a monoclonal antibody against HER2 for metastatic breast cancer that overexpresses HER2. N Engl J Med 2001;344:783–92.
3. Giancotti FG, Ruoslahti E. Integrin signaling. Science 1999;285:1028–32.
4. White DE, Kurpios NA, Zuo D, et al. Targeted disruption of β_1-integrin in a transgenic mouse model of human breast cancer reveals an essential role in mammary tumor induction. Cancer Cell 2004;6:159–70.
5. Berry MG, Gui GP, Wells CA, Carpenter R. Integrin expression and survival in human breast cancer. Eur J Surg Oncol 2004;30:484–9.
6. Gui GP, Wells CA, Yeomans P, et al. Integrin expression in breast cancer cytology: a novel predictor of axillary metastasis. Eur J Surg Oncol 1996;22:254–8.
7. Shaw LM. Integrin function in breast carcinoma progression. J Mammary Gland Biol Neoplasia 1999;4:367–76.
8. Zutter MM, Krigman HR, Santoro SA. Altered integrin expression in adenocarcinoma of the breast. Analysis by *in situ* hybridization. Am J Pathol 1993;142:1439–48.
9. Aoudjit F, Vuori K. Integrin signaling inhibits paclitaxel-induced apoptosis in breast cancer cells. Oncogene 2001;20:4995–5004.
10. Damiano JS. Integrins as novel drug targets for overcoming innate drug resistance. Curr Cancer Drug Targets 2002;2:37–43.
11. Lewis JM, Truong TN, Schwartz MA. Integrins regulate the apoptotic response to DNA damage through modulation of p53. Proc Natl Acad Sci U S A 2002;99:3627–32.
12. Sethi T, Rintoul RC, Moore SM, et al. Extracellular matrix proteins protect small cell lung cancer cells against apoptosis: a mechanism for small cell lung cancer growth and drug resistance *in vivo*. Nat Med 1999;5:662–8.
13. Kawamura T, Endo Y, Yonemura Y, et al. Significance of integrin α_2/β_1 in peritoneal dissemination of a human gastric cancer xenograft model. Int J Oncol 2001;18:809–15.
14. Fujita S, Watanabe M, Kubota T, et al. Alteration of expression in integrin β_1-subunit correlates with invasion and metastasis in colorectal cancer. Cancer Lett 1995;91:145–9.
15. Elliott BE, Ekblom P, Pross H, et al. Anti-β_1 integrin IgG inhibits pulmonary macrometastasis and the size of micrometastases from a murine mammary carcinoma. Cell Adhes Commun 1994;1:319–32.
16. Bissell MJ, Weaver VM, Lelievre SA, et al. Tissue structure, nuclear organization, and gene expression in normal and malignant breast. Cancer Res 1999;59:1757–63s; discussion 1763–4s.
17. Weaver VM, Petersen OW, Wang F, et al. Reversion of the malignant phenotype of human breast cells in three-dimensional culture and *in vivo* by integrin blocking antibodies. J Cell Biol 1997;137:231–45.
18. Liu H, Radisky DC, Wang F, Bissell MJ. Polarity and proliferation are controlled by distinct signaling pathways downstream of PI3-kinase in breast epithelial tumor cells. J Cell Biol 2004;164:603–12.
19. Wang F, Weaver VM, Petersen OW, et al. Reciprocal interactions between β_1-integrin and epidermal growth factor receptor in three-dimensional basement membrane breast cultures: a different perspective in epithelial biology. Proc Natl Acad Sci U S A 1998;95:14821–6.
20. Briand P, Petersen OW, Van Deurs B. A new diploid nontumorigenic human breast epithelial cell line isolated and propagated in chemically defined medium. In Vitro Cell Dev Biol 1987;23:181–8.
21. Hall DE, Reichardt LF, Crowley E, et al. The α_1/β_1 and α_6/β_1 integrin heterodimers mediate cell attachment to distinct sites on laminin. J Cell Biol 1990;110:2175–84.
22. Tomaselli KJ, Damsky CH, Reichardt LF. Purification and characterization of mammalian integrins expressed by a rat neuronal cell line (PC12): evidence that they function as α/β heterodimeric receptors for laminin and type IV collagen. J Cell Biol 1988;107:1241–52.
23. Werb Z, Tremble PM, Behrendtsen O, et al. Signal transduction through the fibronectin receptor induces collagenase and stromelysin gene expression. J Cell Biol 1989;109:877–89.
24. Baselga J, Albanell J, Molina MA, Arribas J. Mechanism of action of trastuzumab and scientific update. Semin Oncol 2001;28:4–11.
25. Ott RL. Introduction to statistical methods and data analysis. 5th ed. Belmont (CA): Duxbury Press; 2001.
26. Wang F, Hansen RK, Radisky D, et al. Phenotypic reversion or death of cancer cells by altering signaling pathways in three-dimensional contexts. J Natl Cancer Inst 2002;94:1494–503.
27. Howlett AR, Bailey N, Damsky C, et al. Cellular growth and survival are mediated by β_1 integrins in normal human breast epithelium but not in breast carcinoma. J Cell Sci 1995;108:1945–57.
28. Lelievre SA, Bissell MJ. Three dimensional cell culture: the importance of microenvironment in regulation of function. In: Meyers RA, editor. Encyclopedia of molecular cell biology and molecular medicine. 2nd ed. New York: Wiley; 2005.
29. Weaver VM, Lelievre S, Lakins JN, et al. Beta4 integrin-dependent formation of polarized three-dimensional architecture confers resistance to apoptosis in normal and malignant mammary epithelium. Cancer Cell 2002;2:205–16.
30. Wennerberg K, Fassler R, Warmegard B, Johansson S. Mutational analysis of the potential phosphorylation sites in the cytoplasmic domain of integrin β_{1A}. Requirement for threonines 788–789 in receptor activation. J Cell Sci 1998;111:1117–26.
31. Yamada KM, Pankov R, Cukierman E. Dimensions and dynamics in integrin function. Braz J Med Biol Res 2003;36:959–66.
32. Gu J, Tamura M, Pankov R, et al. Shc and FAK differentially regulate cell motility and directionality modulated by PTEN. J Cell Biol 1999;146:389–403.
33. Romond EH, Perez EA, Bryant J, et al. Trastuzumab plus adjuvant chemotherapy for operable HER2-positive breast cancer. N Engl J Med 2005;353:1673–84.
34. Truong T, Sun G, Doorly M, et al. Modulation of DNA damage-induced apoptosis by cell adhesion is independently mediated by p53 and c-Abl. Proc Natl Acad Sci U S A 2003;100:10281–6.
35. Cukierman E, Pankov R, Stevens DR, Yamada KM. Taking cell-matrix adhesions to the third dimension. Science 2001;294:1708–12.
36. Schmeichel KL, Bissell MJ. Modeling tissue-specific signaling and organ function in three dimensions. J Cell Sci 2003;116:2377–88.
37. Green SK, Francia G, Isidoro C, Kerbel RS. Anti-adhesive antibodies targeting E-cadherin sensitize multicellular tumor spheroids to chemotherapy *in vitro*. Mol Cancer Ther 2004;3:149–59.
38. St Croix B, Florenes VA, Rak JW, et al. Impact of the cyclin-dependent kinase inhibitor p27Kip1 on resistance of tumor cells to anticancer agents. Nat Med 1996;2:1204–10.
39. Boudreau N, Werb Z, Bissell MJ. Suppression of apoptosis by basement membrane requires three-dimensional tissue organization and withdrawal from the cell cycle. Proc Natl Acad Sci U S A 1996;93:3509–13.

40. Cordes N, Blaese MA, Meineke V, Van Beuningen D. Ionizing radiation induces up-regulation of functional β_1-integrin in human lung tumour cell lines *in vitro*. Int J Radiat Biol 2002;78:347–57.
41. Meineke V, Gilbertz KP, Schilperoort K, et al. Ionizing radiation modulates cell surface integrin expression and adhesion of COLO-320 cells to collagen and fibronectin *in vitro*. Strahlenther Onkol 2002;178:709–14.
42. Rosell R, Fossella F, Milas L. Molecular markers and targeted therapy with novel agents: prospects in the treatment of non-small cell lung cancer. Lung Cancer 2002;38 Suppl 4:43–9.
43. Sledge GW, Jr. HERe-2 stay: the continuing importance of translational research in breast cancer. J Natl Cancer Inst 2004;96:725–7.
44. Ruoslahti E. Integrins as signaling molecules and targets for tumor therapy. Kidney Int 1997;51:1413–7.
45. Giancotti FG. Complexity and specificity of integrin signalling. Nat Cell Biol 2000;2:E13–4.
46. Ojakian GK, Ratcliffe DR, Schwimmer R. Integrin regulation of cell-cell adhesion during epithelial tubule formation. J Cell Sci 2001;114:941–52.
47. Celetti A, Garbi C, Consales C, et al. Analysis of cadherin/catenin complexes in transformed thyroid epithelial cells: modulation by β_1 integrin subunit. Eur J Cell Biol 2000;79:583–93.
48. Gutierrez MC, Detre S, Johnston S, et al. Molecular changes in tamoxifen-resistant breast cancer: relationship between estrogen receptor, HER-2, and p38 mitogen-activated protein kinase. J Clin Oncol 2005;23:2469–76.
49. Clynes RA, Towers TL, Presta LG, Ravetch JV. Inhibitory Fc receptors modulate *in vivo* cytoxicity against tumor targets. Nat Med 2000;6:443–6.
50. Takada Y, Puzon W. Identification of a regulatory region of integrin β_1 subunit using activating and inhibiting antibodies. J Biol Chem 1993;268:17597–601.